MAY 1984 LRP 233/84

COMPUTATION OF SYMMETRIC IDEAL MHD FLOW EQUILIBRIA

S. Semenzato, R. Gruber and H.P. Zehrfeld

COMPUTATION OF SYMMETRIC IDEAL MHD FLOW EQUILIBRIA

S. Semenzato, R. Gruber, H.P. Zehrfeld*

Centre de Recherches en Physique des Plasmas
Association Euratom - Confédération Suisse
Ecole Polytechnique Fédérale de Lausanne
21, av. des Bains, CH-1007 Lausanne/Switzerland

* Max-Planck-Institut für Plasmaphysik, Boltzmannstr. 2,
D-8046 Garching bei München

ABSTRACT

The symmetric ideal magnetohydrodynamic equilibrium equations with flow lead to a nonlinear system of four algebraic equations and one quasilinear partial differential equation. These equations are solved numerically by a continuation method, by a Picard iteration and a finite element approach. The nodal points are redistributed iteratively such that they fall on initially prescribed constant flux surfaces. Different coordinate systems are introduced and applied to a static case. A first application to JET is made.

Contents

1. INTRODUCTION

The problem of symmetric ideal MHD flow equilibria was first considered in astrophysics about 25 years ago [6]. In the field of controlled thermonuclear fusion research it became the object of increased interest in connection with the theoretical study of MHD flow effects on toroidal plasma confinement, in particular on equilibrium [22,21] and on the rate of plasma loss from the magnetic confinement region ([23] and the literature cited in [20]). The latter problem is related to non ideal (resistive) properties of the plasma and is beyond the scope of our paper.

Genuine flow equilibria are those which are connected with a finite contribution of the plasma currents to the equilibrium magnetic field and with plasma inertia, i.e. with non-negligible components of $\rho \underline{v} \cdot \nabla \underline{v}$ in the force-balance equations constituting the conditions for equilibrium. The reason for that is that without this contribution the magnetic field configuration is not affected by flow so that the problem becomes a hydrodynamic one leading to equations which can be solved by integrations along magnetic field lines in a given external magnetic field [5]. Without inertia, on the other hand, flow effects enter the problem only through the source of the corresponding partial differential equation for the magnetic field flux whereas the differential operator itself is exactly the same as for static equilibria. It should further be noted that this is true even if plasma inertia is taken into account but the plasma flow is exactly in the direction of the ignorable coordinate (i.e. purely toroidal flow in the case of axial, and purely helical flow in case of helical symmetry). We are therefore in particular interested in the determination of finite-β plasma flow equilibria which have a non-zero rotational transform of the flow field.

Until one year ago, as far as is known to us, only some analytical results have been made for large aspect ratio cases [3,4]. Only very recently, numerical equilibrium calculations including toroidal flow have been performed by Kerner and Jandl [28]. The authors present a finite element method similar to that utilized by Takeda and Tsunematsu [27] for static equilibria. The main difference is that they choose quadrilateral isoparametric finite elements instead of bilinear ones. As in [27] they redistribute the nodal points iteratively such that they fall on initially prescribed Ψ = constant surfaces. With their formulation they manage to deal with x-points.

Another similar finite element approach is presented in this article which is organized as follows :

Section 2 describes the physical background and contains the basic equations. The computational problem consists in the determination of five unknown functions by three linear and one non linear algebraic equations, and a quasilinear partial differential equation which in the no-flow case reduces to the usual (in the mathematical nomenclature) linear partial differential equation for static equilibria (the Grad-Schlüter-Shafranov equation).

In section 3 we present the numerical methods used to solve these non linear equations and implemented in our computer code CLIO. The main idea consists in performing a continuation method starting from a static equilibrium solution and slowly turning on the flow. To solve the quasilinear partial differential equation, we use a Picard method. One Picard step is effectuated by expanding the flux function Ψ in terms of finite elements [24,25,26]. The grid is iteratively arranged in such a way that at the end of the calculation the grid points fall on previously prescribed Ψ = const. surfaces as proposed by Takeda and Tsunematsu [27]. Formulations for different coordinate systems are presented.

In section 4 we first apply our methods to the static analytic Solov'yov equilibrium solution. It reveals that best results are obtained when using a radial coordinate σ such that the plasma surface becomes a constant σ surface. In a second application we calculate the starting point of the continuation method : a static JET equilibrium solution. Finally, toroidal and poloidal flows are added and limits in the calculation of stationary equilibria are discussed.

In Appendix A we prove some differential geometric and vector analytical theorems on vector fields for the considered cases of symmetry. A coordinate invariant form of the quasilinear partial differential equation for the magnetic flux in cases of symmetry (i.e. if there is one "ignorable" coordinate) is derived. Appendix B contains a table of convers ion factors for the transition from natural units (which are used in this paper) to MKSA units.

2. PHYSICAL PROBLEM

2.1 Basic Equations

We will consider certain classes of final states of an ideally moving plasma which evolves in time according to the hydromagnetic equations of motion

$$\rho\left(\frac{\partial \underline{v}}{\partial t} + \underline{v}\cdot\underline{\nabla}\,\underline{v}\right) = (\underline{\nabla}\times\underline{B})\times\underline{B} - \underline{\nabla}p \tag{2.1}$$

$$\underline{\nabla}\cdot\underline{B} = 0 \tag{2.2}$$

and the conservation equations for magnetic flux, for mass and for entropy

$$\frac{\partial \underline{B}}{\partial t} - \underline{\nabla}\times(\underline{v}\times\underline{B}) = 0 \tag{2.3}$$

$$\frac{\partial \rho}{\partial t} + \underline{\nabla}\cdot\rho\,\underline{v} = 0 \tag{2.4}$$

$$\frac{\partial S}{\partial t} + \underline{v}\cdot\underline{\nabla}S = 0\,. \tag{2.5}$$

In order to obtain a complete description we must add an expression for the entropy S per mass unit in the form of a thermodynamic potential

$$S = S_T(u, 1/\rho) \tag{2.6}$$

with

$$\frac{\partial S_T(u, 1/\rho)}{\partial u} = \frac{1}{T} \tag{2.7}$$

$$\frac{\partial S_T(u, 1/\rho)}{\partial(1/\rho)} = \frac{p}{T} \tag{2.8}$$

where U is the plasma internal energy per unit of mass and T the absolute temperature. All other quantities have their usual meaning.

We use natural units which remove the appearance of unnecessary factors from the equations [1].

We define the plasma to be in a magnetohydrodynamic equilibrium state if the vector fields $\underline{v}$ and $\underline{B}$ and the thermodynamic quantities S, ρ and p (in the Eulerian description) are time-independent. Cases of equilibrium states with $\underline{v} \neq 0$ we call flow equilibria. They are described by the equations

$$\rho\, \underline{v} \cdot \underline{\nabla}\, \underline{v} = (\underline{\nabla} \times \underline{B}) \times \underline{B} \tag{2.9}$$

$$\underline{\nabla} \cdot \underline{B} = 0 \tag{2.10}$$

$$\underline{\nabla} \cdot \rho \underline{v} = 0 \tag{2.11}$$

$$\underline{\nabla} \times (\underline{v} \times \underline{B}) = 0 \tag{2.12}$$

$$\underline{v} \cdot \underline{\nabla} S = 0 \,. \tag{2.13}$$

2.2 Conservation Laws and Related Integrals of Motion

In cases of symmetry due to the existence of corresponding invariants along magnetic field lines the problem of finding solutions of these equations reduces to essentially the consideration of a single quasilinear partial differential equation for the magnetic field flux. The mathematical details of this reduction for either axial or helical (or any other) symmetry we give in the Appendix. Here (and later on for the numerical calculations) we refer to axially symmetric toroidal plasma configurations with the ignorable coordinate ϕ about the z axis

---

*) MKSA-units can be obtained by the replacements $t \to tc$, $\rho \to \rho c^2$, $v \to v/c$, $B \to B/\sqrt{\mu_0}$, $S \to S/(kc^2)$, $U \to U/c^2$ and $T \to kT$, where $c = 2.998 \times 10^8$ m/s, $\mu_0 = 4\pi \cdot 10^{-7}$ Vs/Am and $k = 1.38 \times 10^{-23}$ Ws/deg(K). A complete table of conversion factors is given in Appendix B.

(symmetry axis); by r we denote the distance from this axis (see Fig. 1).

As proved in Appendix A, for any vector field $\underline{A}$ there is a vector analytical relation

$$\frac{1}{r^2}\,\underline{\nabla}\times\left(r^2\,\underline{\nabla}\varphi\times\underline{A}\right)=\underline{\nabla}\cdot\underline{A}\;\underline{\nabla}\varphi. \tag{2.14}$$

If $\underline{A}$ is divergence-free then the vector field $r^2\underline{\nabla}\phi \times \underline{A}$ has the poloidal flux of $\underline{A}$ as a potential. In application to the divergence-free fields $\underline{B}$ and $\rho\underline{v}$ (putting $\underline{A} = \underline{B}$ and $\underline{A} = \rho\underline{v}$, respectively) the representations

$$\underline{B} = \underline{\nabla}\varphi\times\underline{\nabla}\Psi + J\,\underline{\nabla}\varphi \tag{2.15}$$

$$\rho\underline{v} = \underline{\nabla}\varphi\times\underline{\nabla}\Psi_M + L\,\underline{\nabla}\varphi \tag{2.16}$$

can be found, where J and L are auxilliary variables describing the toroidal field components :

$$J = r^2\,\underline{B}\cdot\underline{\nabla}\varphi \tag{2.17}$$

$$L = r^2\rho\,\underline{v}\cdot\underline{\nabla}\varphi\quad) \tag{2.18}$$

Ψ and Ψ_M are the poloidal fluxes of the magnetic induction $\underline{B}$ and of the flow field momentum density $\rho\underline{v}$, respectively *). With $\mathcal{C}_S = \mathcal{C}_S(r,z) = \{(X,Y,Z) : X=r\cos\phi,\ Y=r\sin\phi,\ Z=z;\ \phi\in(0,2\pi)\}$ as the definition of a symmetry line (where (X,Y,Z) are the cartesian components of the position vector $\underline{x}$) the quantity J can be identified by Ampere's law as the poloidal current per radian :

$$J(r,z) = \frac{1}{2\pi}\oint_{\mathcal{C}_S(r,z)}\underline{B}\cdot d\underline{s} \tag{2.19}$$

L is its analogon with respect to the momentum density field $\rho\underline{v}$,

$$L(r,z) = \frac{1}{2\pi}\oint_{\mathcal{C}_S(r,z)}\rho\underline{v}\cdot d\underline{s}\quad. \tag{2.20}$$

---

*) We have introduced them as fluxes per radian.

The irrotational field $\underline{v}\times\underline{B}$ implies the existence of an electric potential Φ (with the electric field $\underline{E} = -\underline{\nabla}\Phi$) of the form $\Phi = \Phi(\Psi)$ so that

$$\underline{v}\times\underline{B} = \Phi'(\Psi)\,\underline{\nabla}\Psi \, . \tag{2.21}$$

Inserting here the representations (2.15) and (2.16) it can be found that Ψ_M is also of the form $\Psi_M = \Psi_M(\Psi)$ and together with $\Phi'(\Psi)$, ρ, L and J must satisfy the relation *)

$$L = J\,\Psi_M' - r^2 \rho\, \Phi' \, , \tag{2.22}$$

i.e. expresses L in terms of the surface quantities Ψ_M and Φ, of the mass density ρ and the poloidal current J. For a closer consideration of relation (2.22) and also for later purposes we introduce the volume $V(\Psi)$ enclosed by the magnetic surface with the flux value Ψ and the usual flux-surface average

$$\langle \dots \rangle = \frac{d}{dV}\iiint\limits_{\underline{\omega}} \dots\, d^3x = \frac{1}{V'(\Psi)}\iint\limits_{\underline{\gamma}=\partial\underline{\omega}} \dots \frac{ds}{|\underline{\nabla}\Psi|} = \frac{\oint_{\gamma} \dots \frac{ds}{B_p}}{\oint_{\gamma} \frac{ds}{B_p}} \tag{2.23}$$

where $\underline{\omega} = \underline{\omega}(V) = \{x=(X,Y,Z) : \Psi(x) < \Psi(V)\}$; ds is the line element along the poloidal cross-sectional contour γ of the considered magnetic surface $\underline{\gamma}$ and $B_p = |\underline{\nabla}\Psi|/r$ is the poloidal magnetic field. $V'(\Psi)$ is given by

$$V'(\Psi) = 2\pi \oint_{\gamma} ds / B_p \, . \tag{2.24}$$

For the inverse rotational transforms (the "safety factors") of the magnetic field and the flow field which are defined as the poloidal flux (the Ψ- and Ψ_M-) derivatives of the corresponding fluxes of

---

*) If no other independent variable is indicated a prime (') denotes the derivative $F' = \underline{\nabla}\Psi \cdot \underline{\nabla}F/|\underline{\nabla}\Psi|^2$, where F is any scalar function. For a surface quantity F_s the total derivative $F_s' = dF_s/d\Psi$ is obtained.

these fields in the toroidal direction, we obtain

$$q = \frac{1}{4\pi^2}\frac{\langle J/r^2\rangle}{\Psi'(V)} = \frac{1}{2\pi}\oint_{\gamma}\frac{J\,ds}{r|\nabla\Psi|} \tag{2.25}$$

$$q_M = \frac{1}{4\pi^2}\frac{\langle L/r^2\rangle}{\Psi_M'(V)} = \frac{1}{2\pi}\oint_{\gamma}\frac{L\,ds}{r|\nabla\Psi|} \quad . \tag{2.26}$$

Dividing (2.18) by r^2 and averaging over a flux surface reveals that the q-values of the magnetic field and of the flow field are related by

$$q_M = q - \frac{\langle\rho\rangle}{4\pi^2}\,\frac{\Phi' V'}{\Psi_M'} \quad . \tag{2.27}$$

2.3 The Equilibrium Problem in Terms of Surface Quantities

The state of the consideration can be summarized as follows :

For any specification of surface quantities Ψ_M and Φ and of space functions $\Psi(\underline{x})$, $\rho(\underline{x})$ and $J(\underline{x})$ the equations (2.10) to (2.12) are satisfied for the fields (2.15) and (2.16) if L is determined through equation (2.22). Anticipating that further equations for the surface quantities Ψ_M and Φ will not be obtained we expect the equations of motion and entropy conservation to determine the as yet know quantities Ψ, ρ, J and S.

Let us begin with the entropy. For purely toroidal flow equation (2.13) imposes no condition on S as $\underline{v} \cdot \underline{\nabla} S = 0$ for any S. We exclude this case for the present and assume a finite value for q_M (or, equivalently, a non-vanishing value for Ψ_M'). Then the dot product of (2.16) with (2.13) restricts the entropy to $S=S(\Psi)$ (yielding this way a third prescribable surface quantity), and we are left with the equations of motion (2.9) as the remaining equations for J, ρ and Ψ. The components parallel to $\underline{B}$ and in toroidal direction can be integrated along field lines and lead to the appearance of two further surface quantities $H_M(\Psi)$ and $J_M(\Psi)$ which are given by

$$H_M(\Psi) = \frac{\Psi_M'^2 B^2}{2\rho^2} - \frac{1}{2}\, r^2 \Phi'^2 + H_T(S, \rho) \tag{2.28}$$

$$J_M(\psi) = \left(1 - \frac{\psi_M'^2}{\rho}\right) J + r^2 \psi_M' \Phi' \;, \qquad (2.29)$$

where H_T is the thermodynamic enthalpy

$$H_T = H_T(S, p) \qquad (2.30)$$

with

$$\frac{\partial H_T(S,p)}{\partial S} = T \qquad (2.31)$$

$$\frac{\partial H_T(S,p)}{\partial p} = \frac{1}{\rho} \qquad (2.32)$$

H_T is the Legendre transform of the internal energy U

$$H_T = U + p/\rho \qquad (2.33)$$

and has the independent variables S and p.

The constancy of H_M on a magnetic surface is related to the circulation-preserving property of an ideal medium in fluid mechanics [2].

The functional difference between J_M and J (which is a surface quantity for static equilibria) expresses the necessary modification of the poloidal current if flow is present. For a closer investigation of its meaning we calculate the current density $\underline{j} = \underline{\nabla} \times \underline{B}$ by taking the curl of (2.15). Taking into account (2.14) (with $\underline{A} = \underline{\nabla}\Psi/r^2$) we find

$$\underline{j} = \underline{\nabla} \times \underline{B} = \underline{\nabla} J \times \underline{\nabla}\varphi + r^2\, \underline{\nabla} \cdot \left(\frac{\underline{\nabla}\Psi}{r^2}\right) \underline{\nabla}\varphi \,. \qquad (2.34)$$

This implies $\underline{j} \cdot \underline{\nabla} J = 0$ so that, in virtue of (2.29), current surfaces J = const. and magnetic surfaces Ψ = const. are in general different from each other.

Eliminating now the pressure p from (2.28) using the thermodynamic relation (2.31) provides us in (2.28) and (2.29) with two relations for ρ and J in terms of the five surface quantities J_M, H_M, S, Ψ and Φ which we symbolically abbreviate as

$$F = (J_M, H_M, S, \Psi_M, \Phi) = F(\Psi) . \tag{2.35}$$

A prescription on $F(\Psi)$ allows the determination of ρ and J as functions of r and z - provided we succeed in determining the r-z dependence of the poloidal magnetic flux Ψ. Now the $\underline{\nabla}\Psi$-component of the equation of motion requires for $\Psi(r,z)$ [3] :

$$\underline{\nabla}\cdot\left(\frac{\underline{\nabla}\Psi}{r^2}\right) + \frac{\rho V_p^2}{B_p^2}\left[B_p B_p' - \underline{\nabla}\cdot\left(\frac{\underline{\nabla}\Psi}{r^2}\right)\right] + \frac{1}{r^2} J J' + p' - \frac{\rho V_T^2}{r} r' = 0, \tag{2.36}$$

where a prime (') denotes the derivative (cf. footnote on p.7) $(\underline{\nabla}\Psi/|\underline{\nabla}\Psi|^2)\cdot\underline{\nabla}$, and where

$$B_p = |\underline{\nabla}\Psi| / r \tag{2.37}$$

$$\underline{V}_T = (J\Psi_M'/\rho - r^2\Phi')\,\underline{\nabla}\varphi \tag{2.38}$$

$$\underline{V}_P = (\Psi_M'/\rho)\,\underline{\nabla}\varphi \times \underline{\nabla}\Psi \tag{2.39}$$

$$J = (J_M - r^2\Psi_M'\Phi')/(1 - \Psi_M'^2/\rho) . \tag{2.40}$$

ρ must be determined as a root of the equation

$$H_M - \frac{1}{2}(|\underline{\nabla}\Psi|^2 + J^2)\Psi_M'^2/r^2\rho^2 + \frac{1}{2} r^2\Phi'^2 - H_T(S,p) = 0. \tag{2.41}$$

Here, as well as in equation (2.36), p must be considered as a function of the independent variables S and ρ and is determined by solving the thermodynamic relation (2.32)

$$\frac{\partial H_T(S,p)}{\partial p} = \frac{1}{\rho} \tag{2.42}$$

for the pressure. Note that there is a further dependence of equation (2.42) on ρ through the poloidal current J (2.40).

In the special case of static equilibria (which is formally obtained by putting $F = F_S = (J_M, H_M, S, 0, 0)$ so that $\underline{v}_P = \underline{v}_T = 0$), (2.36) reduces to the usual equilibium partial differential equation for the poloidal flux

$$\underline{\nabla}\cdot\left(\frac{\underline{\nabla}\psi}{r^2}\right) + \frac{1}{r^2} J J' + p' = 0 . \qquad (2.36')$$

From (2.40) follows $J = J_M$ and from (2.41) $H = H_M$ in that case so that J and p become free surface quantities and the problem reduces to the solution of only one equation. In the general case of flow equilibria, however, for a particular family of surface quantities $F = F(\Psi)$, the equations (2.36), (2.41) and (2.42) represent a coupled set of three equations for the three quantities Ψ, ρ and p. It is clear that due to the required substitutions for B_p, $\underline{v}_p$, $\underline{v}_T$ and J (using (2.37) to (2,40)) and the non linear character of (2.41) and (2.42) this is a very involved set. Carrying through these substitutions another form of (2.36) can be derived which is given by

$$\underline{\nabla}\cdot\left[\left(1-\frac{\psi_M'^2}{\rho}\right)\frac{\underline{\nabla}\psi}{r^2}\right] - \frac{1}{r^2} J J_M' + \rho\left(H_M' - TS'\right) + \underline{v}\cdot\underline{B}\,\psi_M'' - L\Phi'' = 0 , \qquad (2.43)$$

where

$$J = \frac{J_M - r^2\psi_M'\Phi'}{1 - \psi_M'^2/\rho} \qquad (2.44)$$

$$L = J\psi_M' - r^2\rho\,\Phi' \qquad (2.45)$$

$$\underline{v}\cdot\underline{B} = \frac{1}{\rho r^2}\left(\psi_M'|\underline{\nabla}\psi|^2 + JL\right) \qquad (2.46)$$

$$T = \frac{\partial H_T(S,p)}{\partial S} \qquad (2.47)$$

and where again (2.41) and (2.42) are the equations for ρ and p.

The physical problem of finding stationary solutions of the evolution equations (2.1) to (2.5) by solution of the reduced stationary problem (2.36) to (2.42) is obviously strongly dependent on the choice for $F(\Psi)$.

Taking for granted the existence of solutions of the non linear algebraic equations (2.41) and (2.42), (2.36) (or, equivalently, (2.43)) is a quasilinear second-order partial differential equation of the form

$$\mathcal{L}\psi = f(r, \psi, |\underline{\nabla}\psi|, F(\psi)) , \qquad (2.48)$$

where $\mathcal{L}$ is the operator

$$\mathcal{L} \equiv \underline{\nabla} \cdot (D/r^2)\, \underline{\nabla} = \mathcal{L}(r, \Psi, |\underline{\nabla}\Psi|, F(\Psi)) \tag{2.49}$$

with

$$D = 1 - \Psi_M'^2/\rho \tag{2.50}$$

and

$$\mathcal{S} = -\frac{1}{r^2} J J_M' - \rho\left(H_M' - TS'\right) - \underline{v} \cdot \underline{B}\, \Psi_M'' + L\Phi'' \tag{2.51}$$

the source. In view of the dependencies (2.49) of $\mathcal{L}$, the nature of the quasilinear equation (2.48) is determined by the strength Ψ_M' of the poloidal flow. In terms of an appropriate poloidal Mach-number it was investigated elsewhere [4]; for moderate poloidal flow it is elliptic. Corresponding bounds will be given below.

Note that for purely toroidal flow $\mathcal{L}$ reduces to the linear operator for static equilibria and flow effects enter only through the source; absence of poloidal flow is also peculiar due to the abovementioned indetermination of the entropy which must be removed by additional considerations. One approach is to assume $T = T(\Psi)$, i.e. that the temperature is constant on magnetic surfaces. We will not consider that case here but only remark that it can be treated with the above equations if the enthalpy- and the entropy terms are replaced according to

$$H_T \longrightarrow G_T \tag{2.52}$$

$$-\rho TS' \longrightarrow \rho ST' , \tag{2.53}$$

where $G = G_T(T,p)$ is the thermodynamic free enthalpy

$$G_T = H_T - TS . \tag{2.54}$$

We return now to the consideration of genuine flow equilibria with non-zero poloidal rotation. A simplification we afford is the assumption that the plasma behaves as an ideal gas. Its entropy is then given by

$$S = S_T(U, 1/\rho) = \frac{\ln\left(U/\rho^{\gamma-1}\right)}{m(\gamma-1)} \tag{2.55}$$

where γ is the ratio of the specific heats and m the mass of a plasma particle. Putting

$$C(S) = (\gamma-1)\, e^{m(\gamma-1)S} \,, \tag{2.56}$$

we derive from (2.33) for the enthalpy H_T

$$H_T(S,p) = \frac{\gamma C S^{1/\gamma}}{\gamma-1}\, p^{(1-1/\gamma)} \,. \tag{2.57}$$

Equation (2.31) yields the equation of state

$$p = \rho T/m \tag{2.58}$$

and (2.32) the adiabatic law

$$p = C(S)\,\rho^{\gamma} \,. \tag{2.59}$$

The characteristic determinant corresponding to the characteristic manifolds of (2.48) can now be written as

$$\Delta = \frac{D^2\left[D-(1-D)/\beta\right]}{D\left[1-(1-D)/\beta_P\right]-(1-D)/\beta_T} \tag{2.60}$$

β_P and β_T are the obvious resolution of the local β

$$\beta = \gamma p / B^2 \tag{2.61}$$

into poloidal and toroidal parts ($1/\beta = 1/\beta_P + 1/\beta_T$). There are two elliptic regions for $\mathcal{L}$ ($\Delta > 0$) :

$$0 < \psi_M'^2/\rho \leq \beta/(1+\beta) \tag{2.62}$$

and (for $\beta \ll 1$)

$$\frac{\beta}{1+\beta}\left(1+\frac{\beta^2}{(1+\beta)^2\beta_P}\right) < \frac{\psi_M'^2}{\rho} \leq \frac{\beta_P}{\beta}(1+\beta) \,. \tag{2.63}$$

Note that they are separated by a (for usual tokamaks) very narrow intermediate hyperbolic region.

2.4 Treatment of the Source and the Concept of Reference Line Quantities

The source $\mathcal{S}$ (2.51), admitting that the plasma behaves as an ideal gas, becomes

$$\mathcal{S} = -\frac{1}{r^2} J J_M' - \rho H_M' + \frac{\rho^\gamma}{\gamma - 1} C' - \frac{1}{\rho r^2}\left(\Psi_M' |\underline{\nabla}\Psi|^2 + JL\right)\Psi_M'' + L\Phi''. \qquad (2.64)$$

Putting together the relations (2.44) for the poloidal current J, (2.45) for the quantity L, (2.59) for the pressure p, (2.41) for the mass density ρ and (2.48) for the poloidal magnetic flux Ψ, the ideal MHD equilibrium problem with flow requires us to solve for the quoted five unknown functions. They are related through the four algebraic equations

$$J = \left(J_M - r^2 \Psi_M' \Phi'\right) / D \qquad (2.65)$$

$$L = J\Psi_M' - r^2 \rho \Phi' \qquad (2.66)$$

$$p = \rho T / m \qquad (2.67)$$

$$H_M - \frac{1}{2}\left(|\underline{\nabla}\Psi|^2 + J^2\right)\frac{\Psi_M'^2}{r^2\rho^2} + \frac{1}{2} r^2 \Phi'^2 - \frac{\gamma C}{\gamma - 1}\rho^{\gamma - 1} = 0 \qquad (2.68)$$

and the quasilinear partial differential equation (2.48)

$$\mathcal{L}\Psi = \mathcal{S}(r, \Psi, |\underline{\nabla}\Psi|, F(\Psi)) \qquad (2.69)$$

where $\mathcal{S}$ is given by (2.64) and $\mathcal{L}$ by (2.49) to (2.50). The free functions $F = (J_M, H_M, C, \Psi_M, \Phi)$ (C now replacing the entropy S) are constant on Ψ = const. surfaces. They can be prescribed as functions of Ψ. Any solutions of the problem depend on the corresponding choice for $F(\Psi)$, in particular on $F(\Psi)$ the solutions $\rho = \rho(r, \Psi, |\underline{\nabla}\Psi|, F(\Psi))$ and the solvability range of the mass density equation (2.68). In order to express F in terms of quantities which are commonly used for the description of an equilibrium situation, it is convenient to introduce the concept of a reference line (s. Fig. 2). Assuming a nested set of magnetic surfaces with the flux value Ψ_A on the axis and Ψ_B at the plasma boundary, we define a reference line as the poloidal curve

$$\mathcal{C}_R = \{ r, z : \; r = r_R(\psi), \; z = z_R(\psi); \; \psi \in (\psi_A, \psi_B) \}. \tag{2.70}$$

Let f be any quantity defined on Ω. Then we put

$$f_R(\psi) = f\left(r_R(\psi), \; z_R(\psi)\right) \tag{2.71}$$

and, if $f_R(\Psi(r,z)) \neq 0$,

$$\bar f(r,z) = f(r,z) / f_R(\psi(r,z)). \tag{2.72}$$

Let us further introduce the dimensionless quantities

$$M = \frac{\psi_M' B_R}{\rho_R c_{sR}} \tag{2.73}$$

$$E = -\frac{r_R \Phi'}{c_{sR}} \tag{2.74}$$

where c_s is the isentropic velocity of sound which is given by

$$c_s^2 = -1 \Big/ \left(\rho^2 \frac{\partial^2 H_T}{\partial p^2}\right) = \gamma \frac{p}{\rho} . \tag{2.75}$$

Then equation (2.68) can be written as

$$2\bar\rho^2 \frac{\bar\rho^{\gamma-1} - 1}{\gamma - 1} = \left(M^2 + (\bar r^2 - 1) E^2\right)\bar\rho^2 - \bar B^2 M^2, \tag{2.76}$$

where

$$\bar B^2 = (\beta/\beta_P)_R \, \bar B_P^2 + (\beta/\beta_T)_R \, \frac{\bar J^2}{\bar r^2} \tag{2.77}$$

$$\bar J = \frac{1 - \beta_R M^2 + (\beta\beta_T)_R^{1/2} (\bar r^2 - 1) M E}{1 - \beta_R M^2/\bar\rho} . \tag{2.78}$$

Fig. 3 shows the left-hand side of this equation as a function of $\bar\rho^2$. Intersections of the curve shown with the corresponding curve of the right-hand side represent the desired solutions.

As $M^2\bar{B}^2 > 0$ equation (2.76) has no solution if the dashed line is below the left-hand-side curve. If the reference line is such that $\bar{r} < 1$ is possible in Ω then, for sufficiently large E, (2.76) has no solution. It is clear from this consideration that for a given reference line there are only solutions for a restricted class of surface quantities $F(\Psi)$. This difficulty can be avoided by an appropriate choice of this line which leads to a prescribable subset of surface quantities. We will use therefore as reference line the particular curve which is given by

$$\mathcal{C}_R = \left\{ \left(r, z : \psi(r,z) = \psi,\ r = \mathrm{Min}\,! \right),\ \psi \in (\psi_A, \psi_B) \right\} \tag{2.79}$$

Thus $\bar{r} > 1$ in Ω and it can be found that equation (2.76) always has a solution in the first ellipticity region. It has an upper bound, i.e.

$$0 < \bar{\rho} \leq \left[1 + \frac{1}{2}(\gamma - 1)\left(M^2 + (\bar{r}^2 - 1)\,E^2\right) \right]^{1/(1-\gamma)} \tag{2.80}$$

which for M = 0 satisfies equation (2.76) exactly, because it is derived from this equation leaving out the last term.

2.5 Boundary Conditions and Variational Formulation

The plasma region Ω is restricted by a rough rigid infinitely conducting wall at Γ. Here, rough means that we do not allow any flow at the surface of the wall, i.e.

$$(v = 0)\,\big|_\Gamma \tag{2.81}$$

which implies that $\Psi_M' = L = \Phi' = 0$, $D = 1$ and $J = \text{constant}$ at Γ. Since the wall is a perfect conductor, it is a $\Psi = \text{constant}$ surface, the value of the constant (replacing Ψ by $\Psi - \Psi_B$) is set to be zero, i.e.

$$(\psi = 0)\,\big|_\Gamma \quad . \tag{2.82}$$

As the plasma touches the wall, its temperature is very small and the resistivity so high that we require that the toroidal current density

$$\left(j_T = 0 \right) \Big|_{\Gamma} \quad , \tag{2.83}$$

leading to $J_M' = H_M' = C' = C = p = 0$ at Γ.

If the free functions are smooth functions of Ψ, the trivial solution $\Psi = 0$ satisfies the equations. In order to prevent this solution we have to normalize our systems by demanding for instance that the total toroidal current

$$\int_{\Omega} j_T \, d^2x = I \tag{2.84}$$

be imposed. Here d^2x is the area element in Ω and j_T is the toroidal current density which according to equation (2.34) is given by

$$j_T = r \, \underline{\nabla} \cdot \frac{\underline{\nabla}\Psi}{r^2} \quad . \tag{2.85}$$

Thus, as $d^3x = 2\pi r d^2x$

$$I = \int_{\Omega} r \, \underline{\nabla} \cdot \frac{\underline{\nabla}\Psi}{r^2} d^2x = \frac{1}{2\pi} \int_{\underline{\omega}} \underline{\nabla} \cdot \frac{\underline{\nabla}\Psi}{r^2} d^3x = \frac{1}{2\pi} \int_{\underline{\Gamma} = \partial\underline{\omega}} \frac{|\underline{\nabla}\Psi|}{r^2} d^2x \, . \tag{2.86}$$

As D = 1 at the plasma boundary we may equally well write

$$I = \frac{1}{2\pi} \int_{\underline{\omega}} \underline{\nabla} \cdot \frac{D \underline{\nabla}\Psi}{r^2} d^3x = \frac{1}{2\pi} \int_{\underline{\omega}} \mathcal{J} \, d^3x \, . \tag{2.87}$$

In order to solve problems where the total toroidal plasma current I is prescribed we perform a scaling of the five profiles F which leads to a scaling factor λ in front of the source , i.e.

$$\mathcal{J} = \lambda \, \mathcal{J}^* \tag{2.88}$$

where $\mathcal{J}^*$ is the scaled source; λ is determined by the condition that

$$\lambda \int_{\Omega} \mathcal{J}^* r \, d^2x = I \, . \tag{2.89}$$

Let us now introduce U to be the set of all functions $u \in L^2(\Omega)$ ($L^2(\Omega)$ is the set of all square integrable functions in the plasma domain Ω), $\underline{\nabla} u \in L^2(\Omega)$ and $u/\Gamma = 0$. If we multiply (3.5) with a test function $\eta \in U$ and integrate the left-hand side by parts,

$$\int_{\omega} \eta \, \underline{\nabla} \cdot \left(\frac{D}{r^2} \underline{\nabla} \psi \right) d^3x = - \int_{\omega} \frac{D}{r^2} \underline{\nabla} \psi \cdot \underline{\nabla} \eta \, d^3x \qquad (2.90)$$

the problem of finding a solution of (3.5) can be written in its weak form

"Find $\Psi \in U$ such that

$$- \int_{\Omega} \frac{D}{r} \underline{\nabla} \psi \cdot \underline{\nabla} \eta \, d^2x = \lambda \int_{\Omega} \eta \, f^* r \, d^2x \qquad (2.91)$$

for all $\eta \in U$ and, for a given value of I,

$$\lambda \int_{\Omega} f^* r \, d^2x = I \quad ." \qquad (2.92)$$

As it turns out, an effective treatment of the flow equilibrium problem by finite elements using the weak formulation (2.91,92) depends sensitively on an appropriate choice of the coordinates describing the domain Ω.

Let $\underline{x} = (x,y,z)$ be the position vector and $\alpha = (\alpha^1, \alpha^2)$ any curvilinear coordinates in Ω. The $\underline{x}$ has the parameter representation in Ω

$$\underline{x}(\alpha, \varphi) = r(\alpha) \, \underline{\nabla} r + z(\alpha) \, \underline{\nabla} z \, . \qquad (2.93)$$

Note that $\underline{\nabla} r$ is an inhomogeneous gradient field depending on ϕ. In these coordinates we have the relations

$$d^2x = \frac{\sqrt{g}}{r} d^2\alpha = \frac{\sqrt{g}}{r} d\alpha^1 d\alpha^2 \qquad (2.94)$$

and

$$\sqrt{g} = \left(\frac{\partial \underline{x}}{\partial \alpha^1} \times \frac{\partial \underline{x}}{\partial \alpha^2} \right) \cdot \frac{\partial \underline{x}}{\partial \varphi} \qquad (2.95)$$

where $\sqrt{g}$ is the volume element. Thus the formulas in (2.91,92) take the form

$$- \int_{\Omega} \underline{\nabla} \psi \cdot \underline{\nabla} \eta \, \frac{D \sqrt{g}}{r^2} d^2\alpha = \lambda \int_{\Omega} \eta \, f^* \sqrt{g} \, d^2\alpha \qquad (2.96)$$

$$\lambda \int_{\Omega} f^{*} \sqrt{g} \; d^2\alpha = I \; . \tag{2.97}$$

For the evaluation of $\underline{\nabla}\Psi \cdot \underline{\nabla}\eta$ the contravariant components $g^{\mu\nu}$ of the metric tensor $\underline{g}$ are needed, because

$$\underline{\nabla}\Psi \cdot \underline{\nabla}\eta = g^{\mu\nu} \frac{\partial \Psi}{\partial \alpha^{\nu}} \frac{\partial \eta}{\partial \alpha^{\mu}} \qquad (\mu, \nu = 1,2). \tag{2.98}$$

(I) The simplest choice of coordinates in Ω is $\alpha = (r,z)$. We have $\sqrt{g} = r$ and the formulas (2.91,92) read

$$-\int_{\Omega} \frac{D}{r}\left(\frac{\partial \Psi}{\partial r}\frac{\partial \eta}{\partial r} + \frac{\partial \Psi}{\partial z}\frac{\partial \eta}{\partial z}\right) dr\,dz = \lambda \int_{\Omega} \eta \, f^{*} r\,dr\,dz \tag{2.99}$$

$$\lambda \int_{\Omega} f^{*} r\,dr\,dz = I \; . \tag{2.100}$$

(II) A second choice with an exact fit of one of the coordinate lines with a circular plasma boundary is given by

$$\alpha = (\theta, \rho) \qquad \begin{aligned} r &= r_0 + \rho \cos\theta \\ z &= \rho \sin\theta \; . \end{aligned} \tag{2.101}$$

It can be conceived as special case of the following more general parametrization of the poloidal plane :

$$\alpha = (\theta, \sigma) \qquad r = r_0 + \sigma \rho_B(\theta) \cos\theta \tag{2.102}$$

$$z = \sigma \rho_B(\theta) \sin\theta \; , \tag{2.103}$$

where $\rho_B(\theta)$ is the radial distance from the point $(r,z) = (r_0, 0)$ to the plasma boundary. For its geometry it is found that

$$g^{-1} = \begin{pmatrix} g^{\theta\theta} & g^{\theta\sigma} & 0 \\ g^{\theta\sigma} & g^{\sigma\sigma} & 0 \\ 0 & 0 & g^{\varphi\varphi} \end{pmatrix} = \frac{1}{\rho_B^2} \begin{pmatrix} \frac{1}{\sigma^2} & -\frac{\dot{\rho}_B}{\rho_B \sigma} & 0 \\ -\frac{\dot{\rho}_B}{\rho_B \sigma} & 1 + \frac{\dot{\rho}_B^2}{\rho_B^2} & 0 \\ 0 & 0 & \frac{\rho_B^2}{r^2} \end{pmatrix} \tag{2.104}$$

$$\sqrt{g} = r\sigma\rho_B^2 \quad , \quad \dot{\rho}_B = \frac{d\rho_B(\theta)}{d\theta} \quad . \qquad (2.105,106)$$

This gives for (2.96) and (2.97)

$$-\int_\Omega \frac{D\sigma}{r}\left[\psi_\sigma \eta_\sigma + \left(\frac{1}{\sigma}\psi_\theta - \frac{\dot{\rho}_B}{\rho_B}\psi_\sigma\right)\left(\frac{1}{\sigma}\eta_\theta - \frac{\dot{\rho}_B}{\rho_B}\eta_\sigma\right)\right] d\sigma d\theta = \lambda \int_\Omega \eta\, f^* r \rho_B^2 \sigma d\sigma d\theta \qquad (2.107)$$

$$\lambda \int_\Omega f^* r \rho_B^2 \sigma d\sigma d\theta = I \, . \qquad (2.108)$$

Here partial derivatives with respect to the variables θ and σ are abbreviated using corresponding subscripts.

2.6 Choice of Equilibrium Quantity Distributions

Instead fo prescribing the family $F = F(J_M, H_M, C, \Psi_M, \Phi)$ as functions of Ψ we prefer the equivalent prescription of reference line distributions for poloidal current J, mass density ρ, temperature T, poloidal velocity v_P and toroidal velocity v_T, i.e. consider the transformation

$$F(\psi) \rightarrow F_R(\psi) = (J, \rho, T, v_P, v_T)_R \quad . \qquad (2.109)$$

The formulas which yield this transformation are

$$J_R = \frac{J_M - r_R^2 \Phi' \Psi_M'}{1 - \Psi_M'^2/\rho_R} \qquad (2.110)$$

$$H_M = \frac{1}{2}\frac{\Psi_M'^2}{\rho_R^2}\left(B_{PR}^2 + \frac{J_R^2}{r_R^2}\right) - \frac{1}{2} r_R^2 \Phi'^2 + \frac{\gamma C \rho_R^{\gamma-1}}{\rho_R^{-1}} \qquad (2.111)$$

$$\rho_R V_{PR} = B_{PR} \Psi_M' \qquad (2.112)$$

$$r_R \rho_R V_{TR} = L_R = J_R \Psi_M' - r_R^2 \rho_R \Phi' \qquad (2.113)$$

$$\rho_R T_R = m C \rho_R^\gamma \quad . \qquad (2.114)$$

Note that all quantities in these expressions are only functions of Ψ and that, through $B_P = |\nabla\Psi|/r$, the solution Ψ of the quasilinear partial differential equation (2.43) itself enters the transformations.

In the choice of the functions F_R on the reference line one has in the transformation (1.109) to carry over the regularity conditions at the magnetic axis. These regularity conditions imply that each term in the source (eq. 2.64) be finite everywhere in Ω_p and, specifically, be finite at the magnetical axis. This implies that

$$
\begin{aligned}
C' &= \frac{d}{d\psi}\left(p_R\,\rho_R^{-\gamma}\right)\\
\Psi_M'' &= \frac{d}{d\psi}\left(r_R\,\rho_R\,v_{PR}^{*}\right)\\
J_M' &= \frac{d}{d\psi}\left(J_R - r_R\,\Psi_M'\,v_{TR}\right)\\
\Phi'' &= \frac{d}{d\psi}\left[\left(J_R\,v_{PR}^{*} - v_{TR}\right)/r_R\right]\\
H_M' &= \frac{d}{d\psi}\left[\frac{1}{2}\,v_{PR}^{*2}\left(|\nabla\psi|_R^2 + J_R^2\right) - \frac{1}{2}\,r_R^2\,\Phi'^2 + \frac{\gamma}{\gamma-1}\,C\,\rho_R^{\gamma-1}\right]
\end{aligned}
\qquad (2.115)
$$

with

$$
v_{PR}^{*} = v_{PR}\,/\,|\nabla\psi|_R \qquad (2.116)
$$

be finite everywhere in Ω_p.

This implies for example that if one chooses for the free functions $F = F(C,\Psi_M',J_M,\Phi',H_M)$ polynomials in Ψ, the functions $F_R = (p_R, v_{pR}, J_R, v_{TR}, \rho_R)$ on the reference line must be polynomials in $\sqrt{\Psi_A - \Psi}$.

3. NUMERICAL APPROACH

3.1 Input Quantities

Flow equilibrium solutions are determined if one prescribes the form $\rho_B(\theta)$ (eqs 2.102,103) of the plasma boundary Γ, the value of the total plasma current I and the profiles of the five free functions $F_R(\Psi)$ (eq. 2.109) on the reference line ℓ_R (eq. 2.79).

Introducing the new unknown

$$
s = \sqrt{\frac{\Psi_A - \Psi}{\Psi_A}} \qquad (3.1)
$$

which varies from 0 at the magnetic axis to 1 at Γ, the profiles chosen for p_R, v_{PR}^*, J_R and ρ_R are

$$
\begin{aligned}
p_R &= \sum_{i=0}^{n} a_i s^i \\
v_{PR}^* &= \sum_{i=0}^{n} b_i s^i \\
J_R &= \sum_{i=0}^{n} c_i s^i \\
V_{TR} &= \sum_{i=0}^{n} d_i s^i \\
\rho_R &= \sum_{i=0}^{n} e_i s^i .
\end{aligned}
\tag{3.2}
$$

To satisfy the regularity conditions that the quantities (2.115) be finite at the magnetical axis R_M one chooses the parameters a_0, b_0, c_0, d_0 and e_0, and determines a_1, b_1, c_1, d_1 and e_1 by the equations :

$$
\begin{aligned}
a_1 - \gamma a_0 e_1/e_0 &= 0 \\
b_1 + b_0 e_1/e_0 &= -t b_0/r_0 \\
c_1 - r_0 \psi_M' d_1 &= t \psi_M' d_0 \\
-c_0 b_1 - b_0 c_1 + d_1 &= -t \Phi' \\
b_0 c_0^2 b_1 + b_0^2 c_0 c_1 + \gamma a_0 e_1/e_0^2 &= t r_0 \Phi'^2
\end{aligned}
\tag{3.3}
$$

where

$$
r_R (R_M) = r_0 + ts \tag{3.4}
$$

and

$$
\begin{aligned}
\psi_M' (R_M) &= r_0 b_0 e_0 \\
\Phi' (R_M) &= (b_0 c_0 - d_0)/r_0 .
\end{aligned}
\tag{3.5}
$$

The resolution of the system (3.3) of linear equations leads to :

$$
\begin{aligned}
e_1/e_0 &= \frac{-b_0^2 c_0^2 + b_0^2 d_0^2 e_0 r_0^2 - \Phi'^2 r_0^2}{-\gamma a_0/e_0 + b_0^2 c_0^2 + \gamma r_0^2 a_0 b_0^2}\, t/r_0 \\
d_1 &= \frac{(-\Phi' - b_0 c_0/r_0 + \psi_M' b_0 d_0)t - b_0 c_0 e_1/e_0}{1 - r_0 \psi_M' b_0} \\
c_1 &= (t\, d_0 + r_0\, d_1)\, \psi_M' \\
b_1 &= -(t/r_0 + e_1/e_0)\, b_0 \\
a_1 &= \gamma\, a_0\, e_1/e_0
\end{aligned}
\qquad (3.6)
$$

The boundary conditions, eqs (2.81-83) imply that

$$\sum_{i=0}^{n} a_i = \sum_{i=0}^{n} b_i = \sum_{i=0}^{n} d_i = \sum_{i=1}^{n} i\, a_i = \sum_{i=1}^{n} i\, c_i = 0 \quad . \qquad (3.7)$$

For practical reason one imposes the values of ρ_R and J_R at the plasma surface. The number of terms n has to be at least n=4 for p_R and J_R. In all our test cases we choose n=4 and impose $a_3 = b_3 = c_3 = d_3 = e_3 = b_4 = d_4 = c_4 = 0$.

Note that choosing $b_0 = d_0 = 0$ implies $a_1 = b_1 = c_1 = d_1 = e_1 = b_2 = d_2 = 0$ which corresponds to the static case.

3.2 Continuation Method

In the search for a solution of the MHD equilibrium problem with flow, we have to be aware of the fact that eqs (2.91,92) are in general highly non linear. Thus iterative schemes often diverge. To guarantee solutions for certain ranges of parameters we apply the continuation method.

As continuation parameters we choose the coefficients

$$\alpha_T = d_o / c_s \quad \left(c_s = \sqrt{\frac{\gamma \alpha_o}{e_o}} \right)$$

and

$$\alpha_p = Max\,(V_{PR}) \,/\, c_s$$

of the profiles for the toroidal and poloidal flow velocities. The starting point is the static MHD equilibrium solution, which we call Ψ_0 for which $\alpha_T = \alpha_p = 0$. Many computer codes exist to calculate such a solution.

At first, only the toroidal flow is switched on. Knowing the solutions for two particular values of α_T, say $\alpha_{T_{k-1}}$ and α_{T_k}, one can obtain an approximate solution $\Psi_{k+1}{}^0$ by

$$\Psi_{k+1}^{0} = \Psi_k + \frac{\alpha_{Tk+1} - \alpha_{Tk}}{\alpha_{Tk} - \alpha_{Tk-1}} \left(\Psi_k - \Psi_{k-1} \right) . \tag{3.8}$$

This approximate solution $\Psi_{k+1}{}^0$ will be used as an initial guess in a Picard iteration.

A similar procedure is used when poloidal flow is included. One starts the continuation method with the initial solution for the desired value of α_T and for $\alpha_p = 0$. With the fixed value of α_T one then switches on the poloidal flow.

3.3 Picard Iteration

The highly nonlinear problem (2.91,92) in which the source term $\mathcal{J}^*$ (eqs 2.64,88) is determined through eqs (2.65-68) is solved by a Picard iteration. One starts from an initial guess Ψ_k^0 obtained by a continuation method as described. Calling (Ψ_k^l, ρ_k^l, J_k^l, L_k^l, p_k^l, λ_k^l) the approximate solution after l Picard steps, one obtains the solution Ψ_k^{l+1} by solving (see eq. 2.91)

$$-\int_{\Omega} \frac{D_k^{\ell}}{r} \underline{\nabla} \Psi_k^{\ell+1} \cdot \nabla \eta \, d^2x = \lambda_k^{\ell} \int_{\Omega} \eta \, \mathcal{J}_k^{*\ell} \, r \, d^2x \, . \qquad (3.9)$$

This equation (3.9) is the weak form also called the variational form of a linear partial differential equation for Ψ_k^{l+1} and is solved by a finite element approach.

If we know the approximate solution Ψ_k^{l+1} it is possible to calculate ρ_k^{l+1} by solving for the nonlinear algebraic equation (2.76) using a Newton method. Introducing Ψ_k^{l+1} and ρ_k^{l+1} into the linear equations (2.65) to (2.67) enables us to compute J_k^{l+1}, L_k^{l+1} and p_k^{l+1} and, as a consequence, the new source $\mathcal{J}_k^{*l+1}$. We are now ready to correct the eigenvalue by solving

$$\lambda_k^{\ell+1} \int_{\Omega} \mathcal{J}_k^{*\ell+1} \, r \, d^2x = I \, . \qquad (3.10)$$

This iteration procedure is stopped when the eigensolution and the eigenvalue are not altered by more than ε after one Picard step, i.e.

$$\frac{\| \Psi_k^{\ell+1} - \Psi_k^{\ell} \|}{\| \Psi_k^{\ell+1} \|} < \varepsilon \qquad (3.11)$$

and

$$\frac{| \lambda_k^{\ell+1} - \lambda_k^{\ell} |}{| \lambda_k^{\ell+1} |} < \varepsilon \, . \qquad (3.12)$$

3.4 Isoparametric bilinear finite elements

For the approximation of Ψ_k^{l+1} in eq. (3.9) by finite elements we have to introduce a finite dimensional subspace $U_h \in U$. The index h will replace the index k and refers to a certain discretization of the domain Ω. The approximation of Ψ_k^{l+1} is called Ψ_h^{l+1}. Problem (3.9) is then written :

"Find $\Psi_h^{l+1} \in U_h$ such that

$$- \int_\Omega \frac{D_h^l}{r} \underline{\nabla} \Psi_h^{l+1} \cdot \underline{\nabla} \eta_h \, d^2x = \lambda_h^l \int_\Omega \eta_h \mathcal{J}_h^{*l} r \, d^2x \tag{3.13}$$

for all $\eta_h \in U_h$."

We denote by (x,y) any of the coordinate systems discussed in (2.99) to (2.108). The domain Ω is discretized by a quadrangular grid as shown in Fig. 4 for (r,z) coordinates. We refer to a nodal point of the grid by (x_i,y_j) (see Fig. 5). The approximate solution Ψ_h can be expanded in terms of finite elements $e_{ij}(x,y)$

$$\Psi_h^{l+1}(x,y) = \sum_i \sum_j \Psi_{ij} \, e_{ij}(x,y) , \tag{3.14}$$

where Ψ_{ij} are the modal values of Ψ_h^{l+1} situated at the grid points (x_i,y_j), and $e_{ij}(x,y)$ are the basis functions which are unity at the grid points (x_i,y_j) and non-zero only in those quadrangular cells for which the point (x_i,y_j) is an edge point. As a complete set of test functions we choose

$$\eta_{kl}(x,y) = e_{kl}(x,y) . \tag{3.15}$$

In general, each quadrangle looks different (see Fig. 4) and thus all the basis functions $e_{ij}(x,y)$ and the domains of integration are different for each cell. This is the reason why one introduces the so-called isoparametric elements [24,26]. In order to perform the integrals in the same way for all cells one projects each quadrangle on a unit square $0 \leq \xi \leq 1$, $0 \leq \chi \leq 1$ (see Fig. 6) through

$$x(\xi,\chi) = \alpha_1 + \alpha_2\xi + \alpha_3\chi + \alpha_4\xi\chi$$
$$y(\xi,\chi) = \beta_1 + \beta_2\xi + \beta_3\chi + \beta_4\xi\chi \tag{3.16}$$

The eight parameters α_1 to α_4 and β_1 to β_4 are determined by the coordinates x_1 to x_4 and y_1 to y_4.

$$\begin{aligned} \alpha_1 &= x_1 & \beta_1 &= y_1 \\ \alpha_2 &= x_2 - x_1 & \beta_2 &= y_2 - y_1 \\ \alpha_3 &= x_3 + x_1 - x_2 - x_4 & \beta_3 &= y_3 + y_1 - y_2 - y_4 \\ \alpha_4 &= x_4 - x_1 & \beta_4 &= y_4 - y_1 \end{aligned} \tag{3.17}$$

In order to prevent problems concerning integration and uniqueness of the transformation (3.16), we demand that all angles of the quadrangles be smaller than π.

By transforming from (x,y) to (ξ,χ) the surface element becomes

$$dx\,dy = J\,d\xi\,d\chi\,, \tag{3.18}$$

where

$$J = \frac{1}{\frac{\partial\xi}{\partial x}\frac{\partial\chi}{\partial y} - \frac{\partial\xi}{\partial y}\frac{\partial\chi}{\partial x}} = (\alpha_2+\alpha_4\chi)(\beta_3+\beta_4\xi) - (\beta_2+\beta_4\chi)(\alpha_3+\alpha_4\xi) \tag{3.19}$$

is the Jacobian. In these new (ξ,χ) coordinates the derivatives of any quantity A become

$$J\frac{\partial A}{\partial x} = (\beta_3+\beta_4\xi)\frac{\partial A}{\partial\xi} - (\beta_2+\beta_4\chi)\frac{\partial A}{\partial\chi}$$
$$J\frac{\partial A}{\partial y} = -(\alpha_3+\alpha_4\xi)\frac{\partial A}{\partial\xi} + (\alpha_2+\alpha_4\chi)\frac{\partial A}{\partial\chi}\,. \tag{3.20}$$

One has to note that these formulae are still valid when the quadrangle degenerates into a triangle as can happen at the origin of a cylindrical coordinate system.

Such a finite element approach leads to a system of linear equations of the form

$$\underline{A}\underline{x} = \underline{b} \qquad (3.21)$$

where $\underline{x}$ includes all the unknowns Ψ_{ij} introduced in eq. (3.14) and $\underline{b}$ represents the right hand side source term. The matrix A is symmetric and positive definite if D > 0. In our computer code CLIO the system of linear equations (3.21) is solved by successive overrelaxation (SOR).

Knowing the approximation $\Psi_h{}^{l+1}$ of $\Psi_k{}^{l+1}$ we can then calculate the approximations of $\rho_k{}^{l+1}, j_k{}^{l+1}, L_k{}^{l+1}, p_k{}^{l+1}$ and of $\lambda_k{}^{l+1}$ using eqs (2.76,65,66,67 and 3.10).

3.5 Grid Adjustment

For (r,z) coordinates, the grid adjustment is made in the following way :

At the beginning of the calculation we fix the center of the meridian plane to be the origin of the coordinate system. From this point are drawn N_θ constant-θ lines which are cut with Γ. These lines are subdivided into N_ρ equidistant intervals. Points with the same ρ counter are connected (ρ is the radial coordinate). This procedure leads to a discretization into quadrangles as shown in Fig. 4a. We are now ready to start Picard's iteration. After a few Picard steps, the mesh is readjusted. The center of the mesh is displaced such that it falls on the magnetic axis. From this new grid center we again draw straight θ = constant lines which are cut with the constant Ψ surfaces. This is obtained by interpolation.

At the end of Picard's iteration we obtain a grid such that all the nodal points fall on the initially prescribed Ψ surfaces. As an example we show in fig. 4b how the initial grid (Fig. 4a) looks after convergence is obtained.

With such a solution it is easy to calculate surface quantities such as the safety factor $q(\Psi)$ or the Mercier criterion and to map from (x,y) into (Ψ,θ) coordinates as used in stability codes such as ERATO [29].

An overall view of all these iteration steps is given in Fig. 7.

3.6 Optimal Coordinates

To find out which one of the coordinate systems discussed in (2.99) to (2.108) is most advantageous, we solve the analytic Solov'yov solution of the static Grad-Schlüter-Shafranov equation (2.36') numerically and compare the obtained results. Choosing as profiles

$$\frac{dp}{d\psi} = \frac{2\psi_A(1+E^2)}{a^2E^2}$$
$$\frac{dJ^2}{d\psi} = 0 \tag{3.22}$$

and Γ of the form

$$\frac{r_B^2 z_B^2}{E^2} + (r_B^2-1)^2/4 = a^2, \tag{3.23}$$

eq. (2.36') is satisfied by

$$\psi = \psi_A - \frac{\psi_A}{a^2}\left[\frac{r^2z^2}{E^2} + (r^2-1)^2/4\right]. \tag{3.24}$$

Here, E and a measure the elongation and the inverse aspect ratio. The position of the magnetic axis is $(r,z) = (1,0)$ at which point $\Psi = \Psi_A$. At Γ, $\Psi = 0$ and $\Psi < 0$ in Ω.

Let us now apply our finite element method with grid adjustment to this Solov'yov test case using (r,z), (ρ,θ) and (σ,θ) as coordinate systems. As parameters we choose $a = 0.25$, $\Psi_A = -E/32$ and the two values $E = 1$ and $E = 2$. The final solutions $\Psi_h(r,z)$ for an (8x8) grid and the two ellipticities are shown in Figs 8a and 8b. One sees that each Ψ = constant surface is strongly deformed. As a consequence, the convergence curves shown in Figs 9a and 9b of the approximated value of Ψ_A are very steep. This poor representation of the solution has already been observed by Takeda and Tsunematsu [27].

It was assumed that a (ρ,θ) coordinate system would improve the situation. The grid adjusted solutions $\Psi(\rho,\theta)$ for the two ellipticities are shown in Figs 8c and 8d. One sees that for E = 1 the ρ-coordinate does not vary strongly as a function of θ. As a consequence, the steepness of the convergence curve for E = 1 shown in Fig. 9a is much smaller than that using a (r,z) grid. In Fig. 10c the solution given in Fig. 8c is replotted in the (r,z) plane. One recognizes the superiority of the solution $\Psi(\rho,\theta)$ compared with $\Psi(r,z)$ represented in Fig. 8a.

However, when we repeat the calculation for an elongated shape we find that a (ρ,θ) grid again distorts the solution (see Fig. 8d). The steepness of the convergence curve shown in Fig. 9b is as large as that for (r,z) coordinates and the representation of the solution $\Psi(\rho,\theta)$ in the (r,z) plane (Fig. 10d) looks quite wrong. We can conclude for a general geometry that both, (r,z) and (ρ,θ) coordinates strongly distort the solution for a coarse mesh.

The use of (σ,θ) coordinates as introduced in (2,102,103) has the great advantage that Γ is always described by

$$\Gamma : \sigma = 1 \tag{3.25}$$

In Figs 8e and 8f are shown the Ψ-mesh adjusted solutions $\Psi(\sigma,\theta)$ for the two ellipticities leading to the representations in the (r,z) plane as plotted in Figs 10e and 10f. These solutions look very good and it is not surprising that the convergence behaviours of Ψ_A as a function of the number of intervals in σ and θ shown in Fig. 9 are very flat. This means that good precision of $\Psi(\sigma,\theta)$ can be obtained with only a few mesh cells.

As a consequence, we use (σ,θ) coordinates for the discretization of the domain Ω and reject both (r,z) and (ρ,θ) coordinates.

4. APPLICATION TO JET

4.1. Input Parameters and Static Equilibrium Solution

The Joint European Tours (JET) is a tokamak built under the auspices of EURATOM. It produced its first plasma in summer 1983. The dimensions of the machine are indicated in Fig. 11. For the plasma surface Γ of JET we have chosen (*).

$$\tilde{r}_B = r_B / R_o = 1 + a \cos(\theta + \Delta \sin\theta)$$
$$\tilde{z}_B = z_B / R_o = E\, a \sin\theta \, . \qquad (4.1)$$

Here, (r_B, z_B) are the real JET surface coordinates and $(\tilde{r}_B, \tilde{z}_B)$ the normalized ones. The major torus radius $R_o = 2.96$ m has been taken as normalization distance. The inverse aspect ratio, the ellipticity and the triangularity are $a = 0.423$, $E = 1.68$ and $\Delta = 0.3$ respectively.

The dimensionless total toroidal current is set to $I = 0.5822$. This current corresponds to a JET current of $IB_oR_o/\mu_o = 4.8$ MA, if $B_o = 3.5$ T.

The additional parameters are chosen such that the volume average beta (eq. 2.61) be $\beta \sim 3$ % which corresponds to the ideal stability limit found by Troyon et al. [31].

(*) In this chapter, besides the natural units, we additionally normalize the distances with R_o which is the major plasma radius (for example $R_o = 2.96$ for JET) and the magnetic fields with the toroidal magnetic field B_o at the position R_o (for example $B_o = 3.5$ T for our JET case). One then obtains dimensionless units. The normalization factors are given in Appendix B.

The static equilibrium problem is obtained when setting :

$$\alpha_T = \alpha_p = 0 . \qquad (4.2)$$

For this case only the profiles for p_R and J_R shown in Fig. 12 have to be given. It is solved using the formerly discussed (σ,θ) coordinates. The initial discretization of the (σ,θ) plane is an equidistant 8 x 8 mesh. The iterative readjustment of the grid leads to a final mesh as shown in Fig. 13. The horizontal curves show equidistant Ψ = constant surfaces. Remember that $\sigma = 0$ denotes the magnetic axis and $\sigma = 1$ is the plasma surface. One sees in Fig. 13 that the Ψ = constant curve closest to $\sigma = 1$ is distorted coming from the fact that x-points lie in the vacuum region close to the plasma surface at $\theta = 3\pi/\Psi$ and $5\,\pi/\Psi$. At these θ values the distortions are most pronounced.

The convergence properties of this static equilibrium solution are plotted in Fig. 14. The straight line of Ψ_A as a function of the number N of intervals in σ and θ shows a quadratic convergence towards $\Psi_A = -2.2282$. This value corresponds to that obtained with a finite differences (r,z) code (EQLAUS) which uses the method described in ref. [30]. The flux surfaces pattern using a 32 x 32 grid is shown in Fig. 15.

Here, the converged solution in the (σ,θ) plane has been represented in the (r,z) plane without performing any additional fitting.

4.2. Influence of Toroidal and Poloidal Flow

As seen before, if flow is on, the flux surfaces and the isobars do not further coincide.

Besides the magnetic axis R_M we can then define a pressure axis R_p which is given by the radial position of the maximum of p on the meridian plane. Note that $R_p = R_M$ if $\alpha_T = \alpha_p = 0$. In the first step only toroidal flow is added. We fix $\alpha_p = 0$ and raise α_T from

0 to 1 which corresponds to a toroidal Mach number of $M_T = 1$.

In Fig. 16 are represented the relative shifts $\Delta R_M/R_M$ and $\Delta R_p/R_p$ as a function of α_T. One sees that the outward shift of R_p is larger than that of R_M.

We have to mention here that $\alpha_T = 1$ is not a limit. The fact that there is no limitation in α_T comes from the fact that pure toroidal flow only modifies the source term $\mathcal{f}^*$ in eq. (3.43) and does not alter the operator which remains elliptic and linear. For a toroidal Mach number of 0.7 and $\alpha_p = v_{pR} = 0$, we have represented the radial profiles on the meridian plane of J_R, ρ_R, p_R and v_{TR} in Fig. 17. The profiles for J_R and p_R can be compared with those given in Fig. 12 for the static equilibrium case. Figure 18 shows the flux surfaces and the isobars (dotted curves) for the same case.

As a next step, we add poloidal flow fixing $\alpha_T = 0.7$. In Fig. 19 are studied the relative changes of R_M and R_p as a function of the poloidal flow α_p. One sees that poloidal flow introduces a strong deformation of the radial profiles on the meridian plane as shown in Fig. 20 for $\alpha_p = 0.12$. For this case, we represent in Fig. 21, the profiles of the five free functions $F(\Psi) = (J_M, H_M, C, \Psi'_M, \Phi')$ versus s.

ACKNOWLEDGEMENTS

We are greatly indebted to Professor F. Troyon for his critics, suggestions and encouragements throughout the whole work. This work has been supported by the Swiss National Science Foundation.

REFERENCES

[1] E.S. Weibel, "Dimensionally Correct Transformation between Different Systems of Units", American Journal of Physics, vol. 36, No. 12, 1130-1133 (1968)

[2] C. Truesdell, R. Toupin, "The Classical Field Theories", Handbuch der Physik, vol. III/1, Springer-Verlag, Berlin (1960)

[3] H.P. Zehrfeld, B.J. Green, "Stationary Toroidal Equilibria at Finite Beta", Nuclear Fusion 12 (1972), 569-575

[4] B.J. Green, H.P. Zehrfeld, "The Effect of Plasma Flow on the Toroidal Equilibrium Shift", Nuclear Fusion 13 (1973), 750-752

[5] H.P. Zehrfeld, B.J. Green "Effect of Inertial on Losses from a Plasma in Toroidal Equilibrium", Nuclear Fusion 10 (1970), 251-258

[6] L. Woltjer, Astrophys. J. 130 (1959), 405

[7] L.S. Solov'yov, Reviews of Plasma Physics (Editor M.A. Leontovich), Consultants Bureau (1967), vol. 3, p. 227

[8] T. Taniuti, Phys. Rev. Letters 25 (1970), 1478

[9] R. Lüst, A. Schlüter, Zeitschrift für Naturforschung 12a, 850 (1957)

[10] N. Asano, T. Taniuti, Phys. Fluids 15 (1972), 423

[11] L.S. Solov'yov, "Symmetric Relativistic MHD-Flows", Fizika Plasmy vol. 6, 2 (1980), 291

[12] E.K. Maschke, H. Perrin, "Exact Solutions of the Stationary MHD Equations for a Rotating Toroidal Plasma", Report EUR-CEA-FC-1022, 1979

[13] E. Hameiri, "Equilibrium and Stability of a Rotating Plasma", Phys. Fluids 26 (1983), 230

[14] N.M. Zueva, L.S. Solovyov, "Change of Magnetic Field Geometry in a Moving Plasma", ZHTF (Letters) 1/24 (1975), 1117

[15] A.G. Oleinik, "Conditions for Toroidal Equilibrium of a Streaming Plasma", PMTF vol. 1 (1976), 31-35

[16] E. Hameiri, "The Stability of a Particular MHD Equilibrium with Flow", NYU-Report COO-3077-123, MF-85 (1976)

[17] J.V. Brackbill, "Computation of Magnetohydrodynamic Flow in a Magnetically Confined Plasma", Nucl. Sci.-Eng., vol. 64/1 (1977), 18

[18] S.S. Gangwar et al., "On the Geometrization of the Steady and Non-dissipative Magnetofluid Flows", Il Nuovo Cim. (B), vol. 54/2 (1979), 349

[19] R. Smith, "Two-Dimensional Hypersonic Magnetohydrodynamic Flow", Phys. Fluids 18 (1975), 40

[20] B.J. Green, "The Effect of Plasma Flow on Toroidal Confinement", Nuclear Fusion 12 (1972), 475

[21] H. Tasso, B.J. Green, H.P. Zehrfeld, "Stationary Equilibrium for the Toroidal Theta Pinch", Phys. Fluids 12 (1969), number 11

[22] J.M. Greene, E.T. Karlson, "A Variational Principle for Stationary Magnetohydrodynamic Equilibria", Princeton Plasma Physics Laboratory, Phys. Fluids 12, 561 (1969)

[23] D. Pfirsch, A. Schlüter, MPI/PA/7/62 (1962)

[24] D.C. Zienkievicz, "The Finite Element Method", 3rd ed. (Mc Graw Hill, London, 1977)

[25] G. Strang, G. Fix, "An Analysis of the Finite Element Method", Series in Automatic Computation (Prentice Hall, 1973)

[26] H.R. Schwarz, "Methode der finiten Elemente", (Teubner, Stuttgart, 1980)

[27] T. Takeda, T. Tsunematsu, "A Numerical Code SELENE to calculate Axisymmetric Equilibria", JAERI-M8042 (1979)

[28] W. Kerner, O. Jandl, "Axisymmetric MHD Equilibria with Flow", Report of the Max-Planck-Institut für Plasmaphysik IPP 6/230 (1983)

[29] R. Gruber et al., "ERATO Stability Code", Computer Phys. Comm. 21 (1981), 323

[30] J.D. Callen, R.A. Dory, Phys. Fluids 15 (1972), 1523

[31] F. Troyon, R. Gruber, H. Saurenmann, S. Semenzato and S. Succi, Plasma Phys. 26, 1A (1983), 209

FIGURE CAPTIONS

Fig. 1 : cylinder co-ordinates (r,ϕ,z) and schematic indication of the current J and the fluxes Ψ and Ψ_M used in the text. Ω is the intersection of the considered (three-dimensional) plasma region with the (r-z)-plane.

Fig. 2 : a reference line leading from the magnetic axis (A) to the plasma boundary (B).

Fig. 3 : left-hand side (L.H.S.) and right-hand side (R.H.S.) of equation (2.76)

Fig. 4 : initial mesh (4a) and final mesh (4b) in the (r,z) plane. The nodal points in (4b) fall on Ψ = constant surfaces.

Fig. 5 : the quadrangular (i,j) cell.

Fig. 6 : transformation from a quadrangular cell in the (x,y) plane to a unit square in the (ξ,χ) plane.

Fig. 7 : instruction flow to solve the ideal stationary MHD equilibrium equations.

Fig. 8 : the (r,z), (ρ,θ) and (σ,θ) meshes for E = 1 and E = 2 and an 8 x 8 grid for the Solov'yov equilibrium test case.

Fig. 9 : convergence study of the maximum value of $|\Psi| = |\Psi_A|$ for the Solov'yov solution and E = 1 (9a) and E = 2 (9b) for (r,z), (ρ,θ) and (σ,θ) coordinates.

Fig. 10 : pattern of the flux surfaces of the Solov'yov solution using an 8 x 8 grid. E = 1 and 2. The solution is calculated in (r,z), (ρ,θ) and (σ,θ) coordinate systems (Fig. 8) and represented in the (r,z) plane.

Fig. 11 : JET geometry.

Fig. 12 : J, p and current density profiles for the static JET equilibrium.

Fig. 13 : the final 8 x 8 grid in the (σ,θ) plane for JET. Horizontal curves are on Ψ = constant surfaces.

Fig. 14 : convergence study of the maximum value of $|\Psi|$ for JET. Quadratic convergence towards $\Psi_A = -2.2282$ is found with CLIO as with the finite difference (r,z) code EQLAUS.

Fig. 15 : the finite element solution for the static JET equilibrium calculated in a 32 x 32 (σ,θ) grid represented in the (r,z) plane.

Fig. 16 : relative shifts $\Delta R_M/R_M$ (curve A) and $\Delta R_p/R_p$ (curve B) and versus the toroidal flow parameter α_T. For $\alpha_p = v_p = 0$. The reference values are those of the static case.

Fig. 17 : radial profiles of J_R, ρ_R, p_R, V_{tR} and current density on the meridian plane for a toroidal Mach number of 0.7 and $\alpha_p = v_p = 0$.

Fig. 18 : for a toroidal Mach number of 0.7 and no poloidal flux, are represented the flux surfaces (solid lines) and the isobars (dotted curves) with locations of the magnetic axis (x sign) and pressure axis (+ sign).

Fig. 19 : for fixed toroidal Mach number = 0.7, are shown the relative shifts $\Delta R_M/R_M$ (curve A) and $\Delta R_p/R_p$ (curve B) versus the poloidal flow parameter α_p. The reference values are those of the static case.

Fig. 20 : radial profiles of J_R, ρ_R, p_R, v_{tR}, v_{pR} and current density on the meridian plane for toroidal and poloidal Mach numbers of respectively 0.7 and 0.12.

Fig. 21 : free functions J_M, C, H_M, Ψ'_M, Φ' versus $s = \sqrt{(\Psi_A - \Psi)/\Psi_A}$ for the $\alpha_T = 0.7$, $\alpha_p = 0.12$ case.

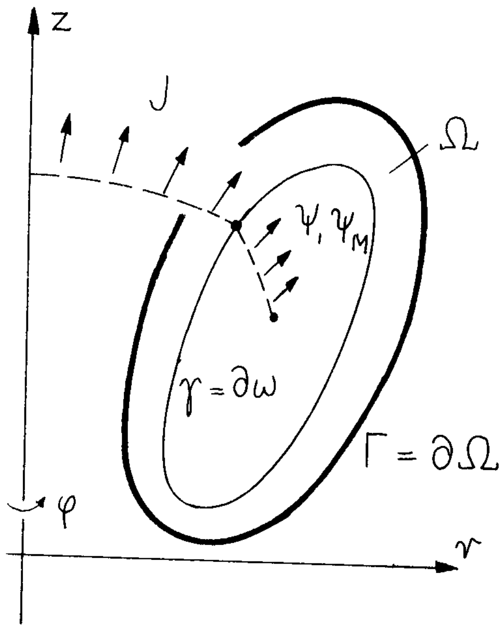

FIG. 1

FIG. 2

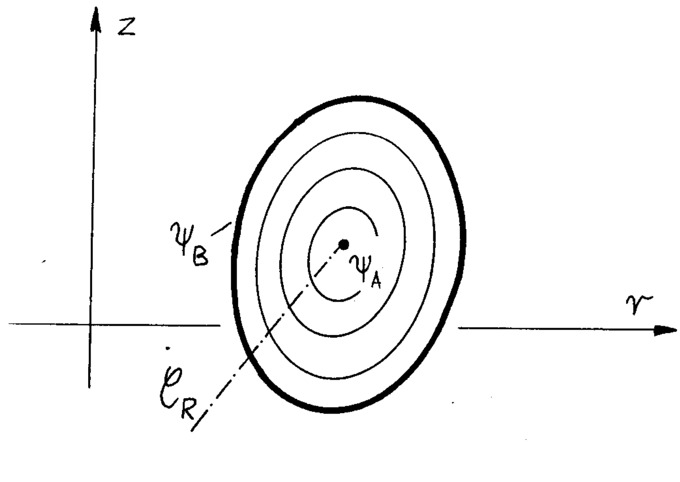

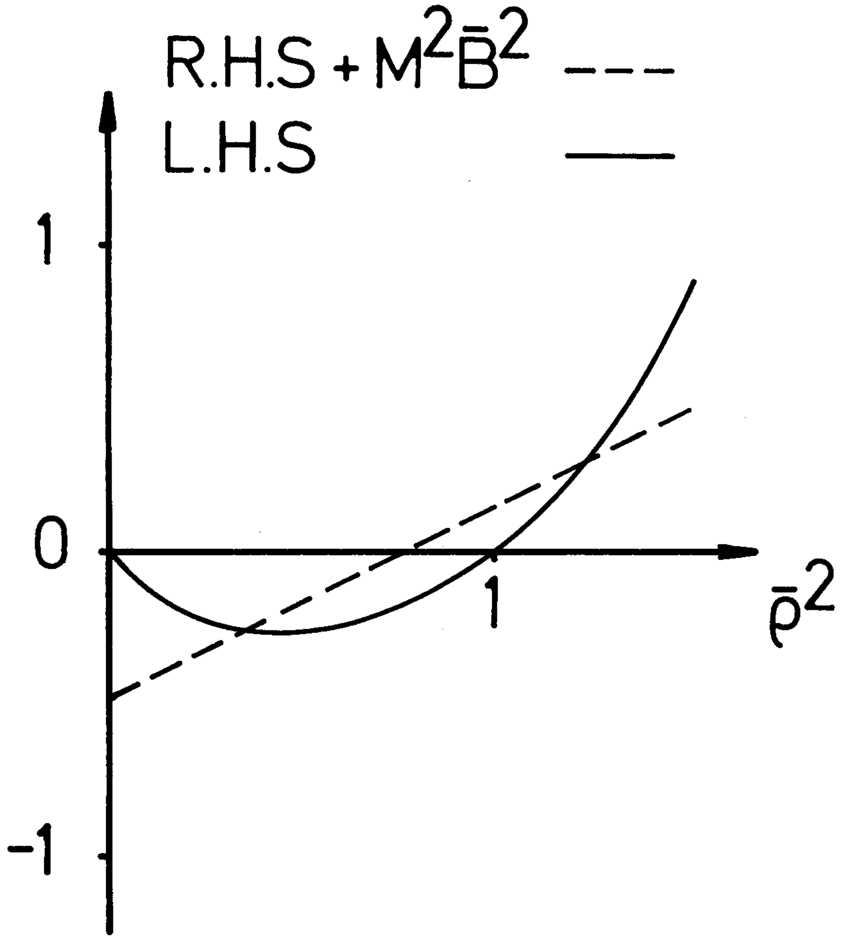

FIG. 3

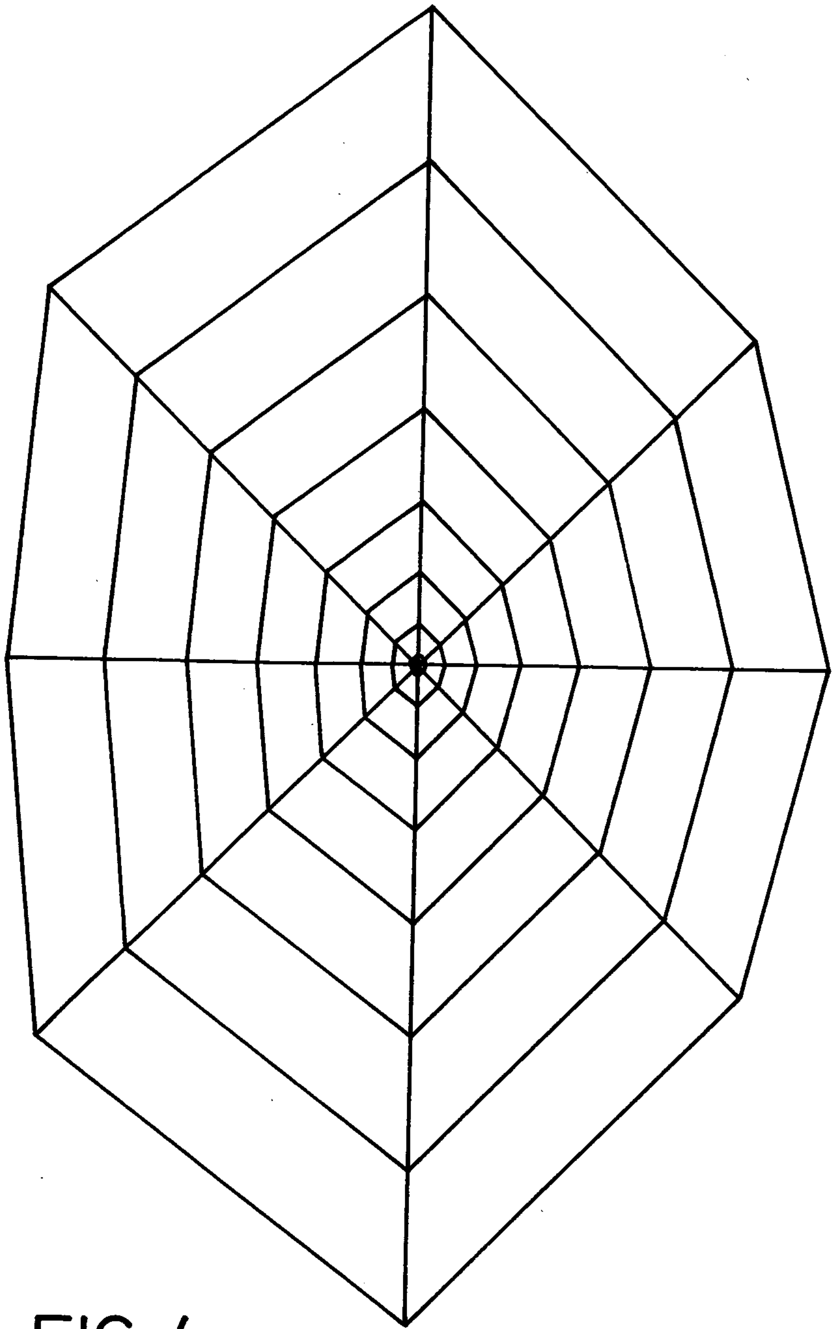

FIG. 4a

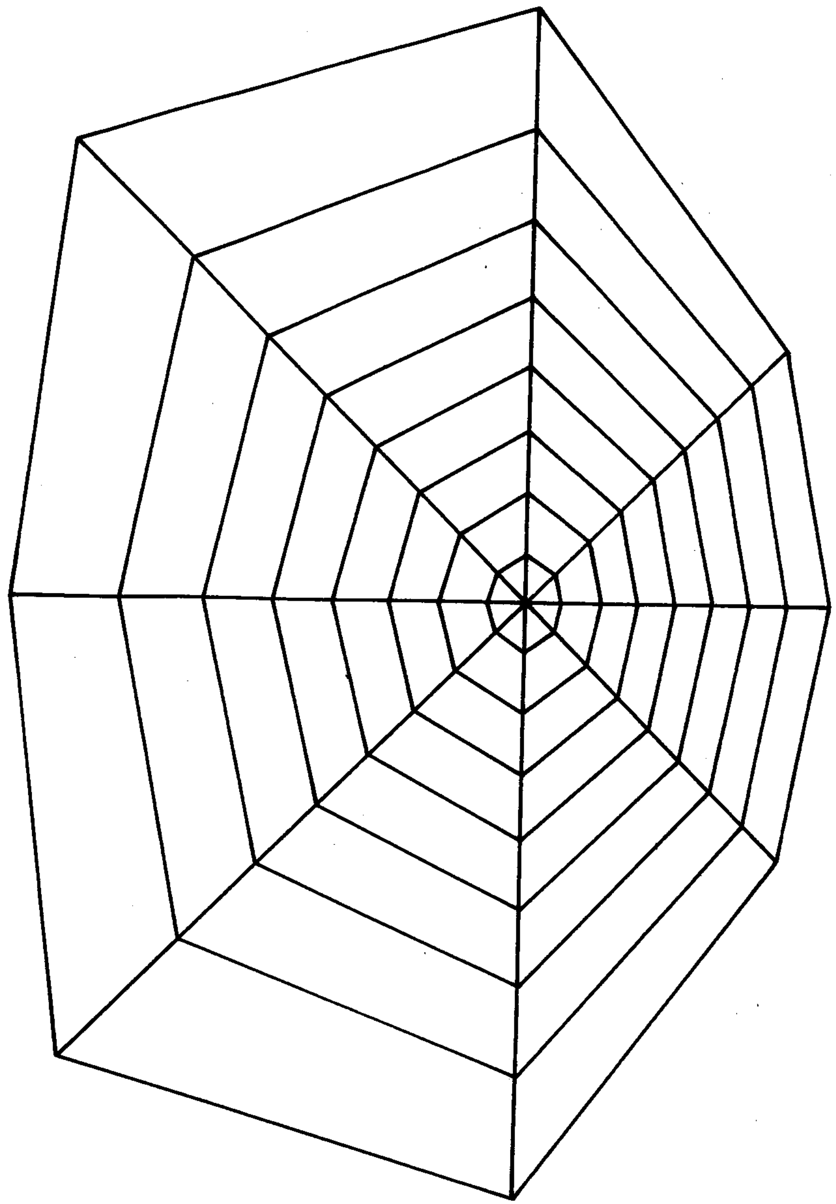

FIG. 4b

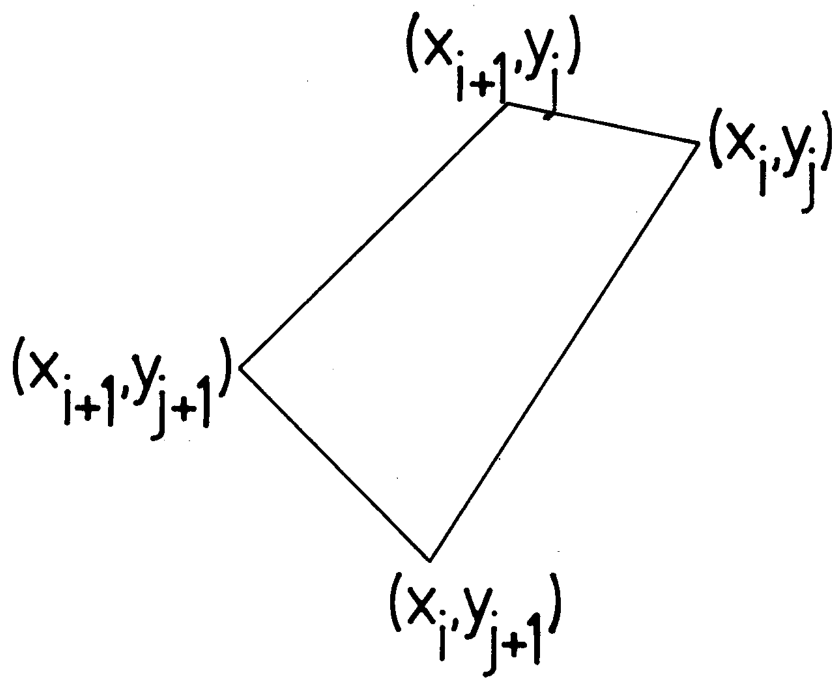

FIG. 5

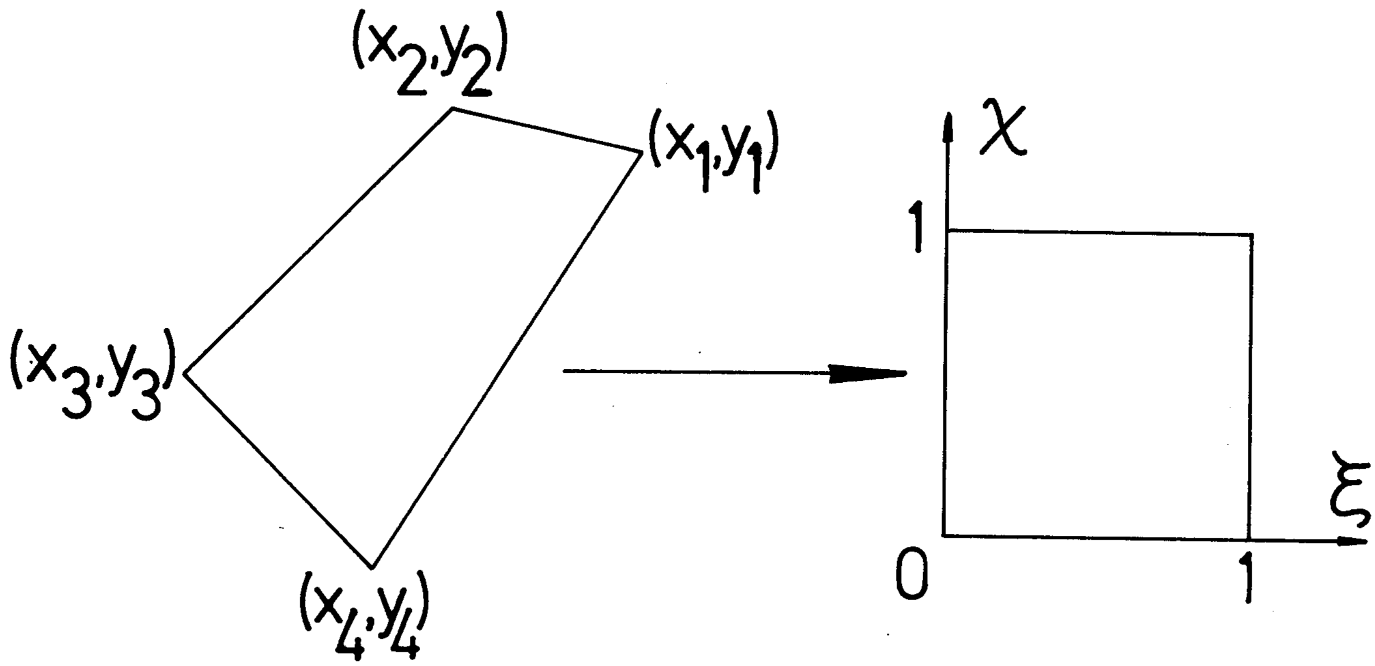

FIG. 6

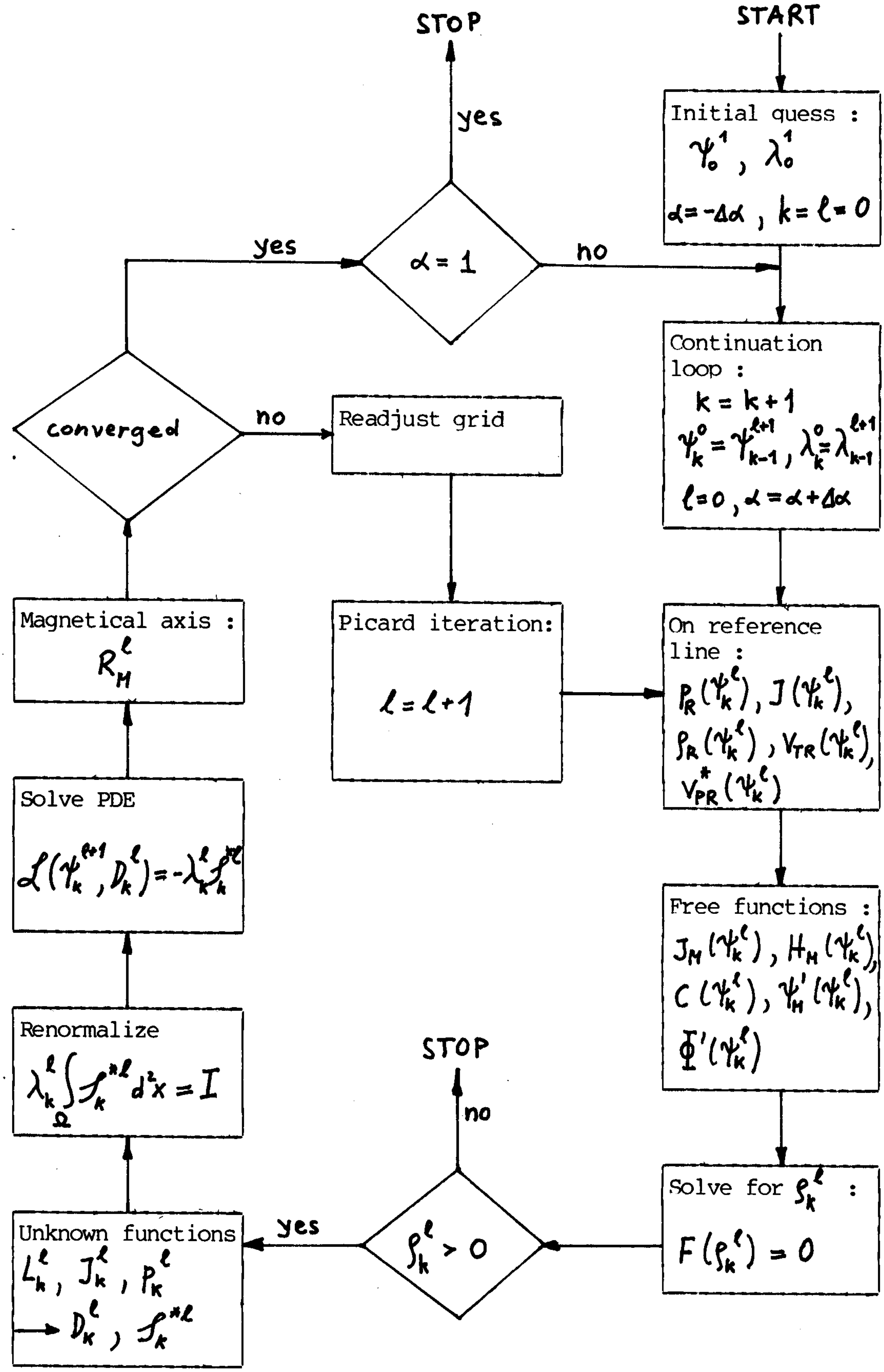
START
Initial guess :
ψ_0^1 , λ_0^1
$\alpha = -\Delta\alpha$, $k = \ell = 0$
Continuation loop :
$k = k+1$
$\psi_k^0 = \psi_{k-1}^{\ell+1}$, $\lambda_k^0 = \lambda_{k-1}^{\ell+1}$
$\ell = 0$, $\alpha = \alpha + \Delta\alpha$
On reference line :
$P_R(\psi_k^\ell)$, $J(\psi_k^\ell)$,
$\rho_R(\psi_k^\ell)$, $V_{TR}(\psi_k^\ell)$,
$V_{PR}^*(\psi_k^\ell)$
Free functions :
$J_M(\psi_k^\ell)$, $H_M(\psi_k^\ell)$,
$C(\psi_k^\ell)$, $\psi_M'(\psi_k^\ell)$,
$\Phi'(\psi_k^\ell)$
Solve for ρ_k^ℓ :
$F(\rho_k^\ell) = 0$
$\rho_k^\ell > 0$
no
STOP
yes
Unknown functions
L_k^ℓ , J_k^ℓ , P_k^ℓ
$\rightarrow D_k^\ell$, $\mathcal{J}_k^{*\ell}$
Renormalize
$\lambda_k^\ell \int_\Omega \mathcal{J}_k^{*\ell} d^2x = I$
Solve PDE
$\mathcal{L}(\psi_k^{\ell+1}, D_k^\ell) = -\lambda_k^\ell \mathcal{J}_k^{*\ell}$
Magnetical axis :
R_M^ℓ
converged
no
Readjust grid
Picard iteration:
$\ell = \ell + 1$
yes
$\alpha = 1$
yes
STOP
no

Fig. 7

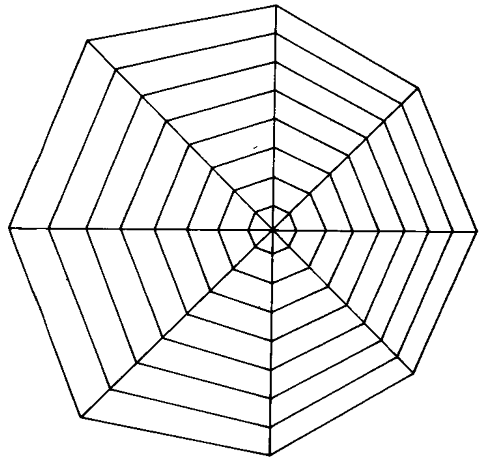

FIG. 8a (r,z) E=1

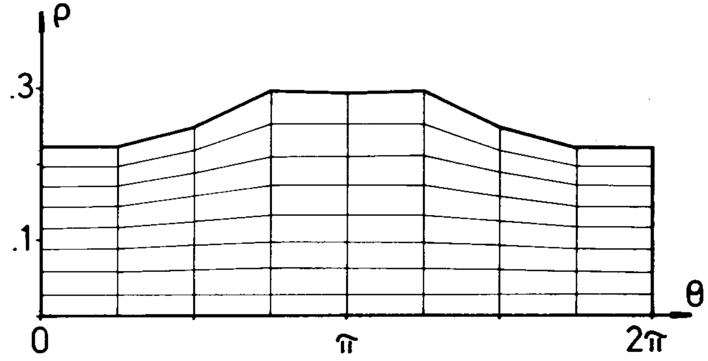

FIG. 8c E=1

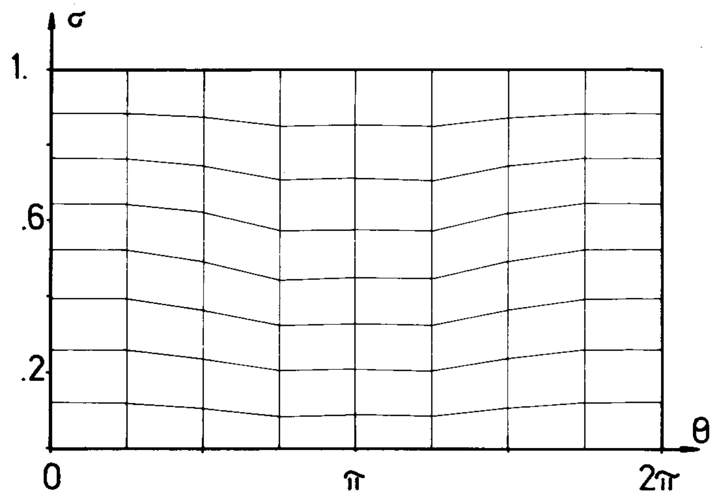

FIG. 8e E=1

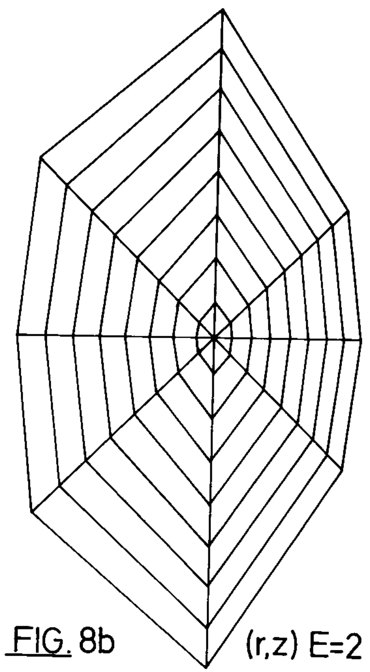

FIG. 8b (r,z) E=2

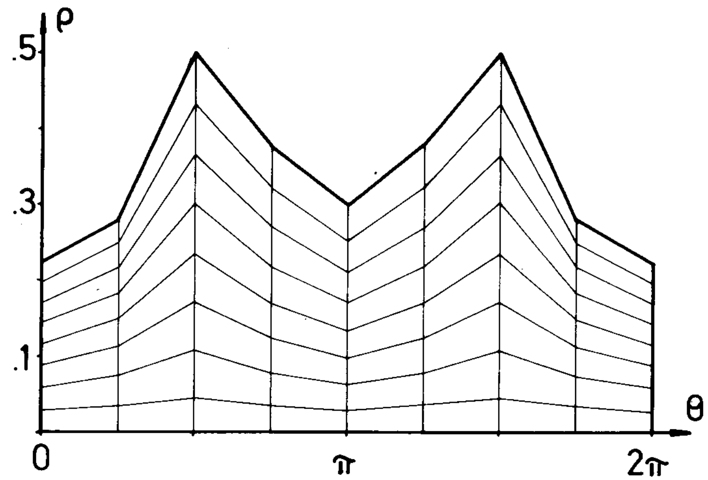

FIG. 8d E=2

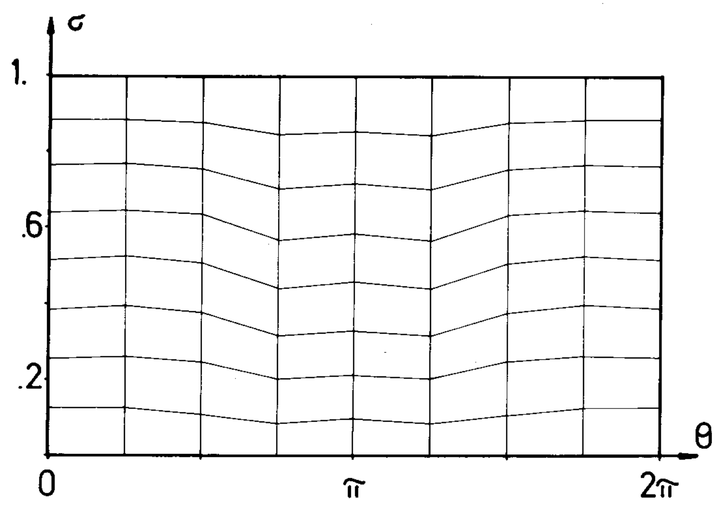

FIG. 8f E=2

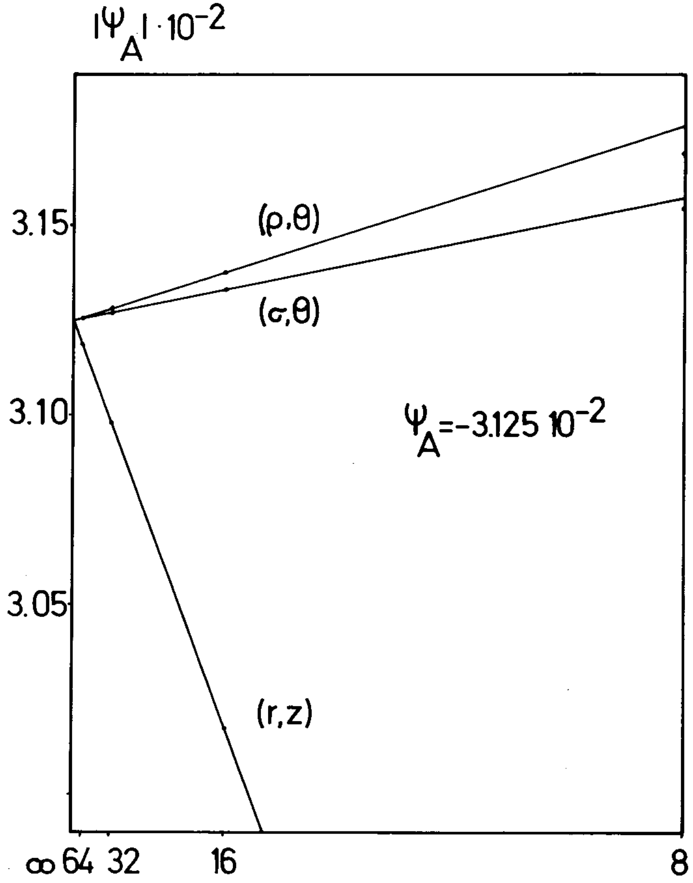

FIG. 9a E=1

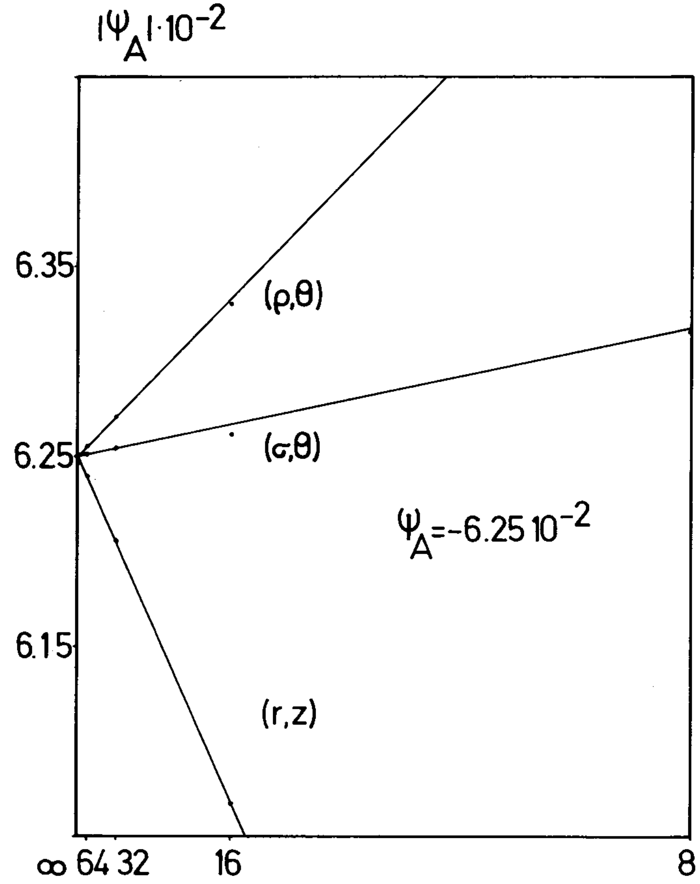

FIG. 9b E=2

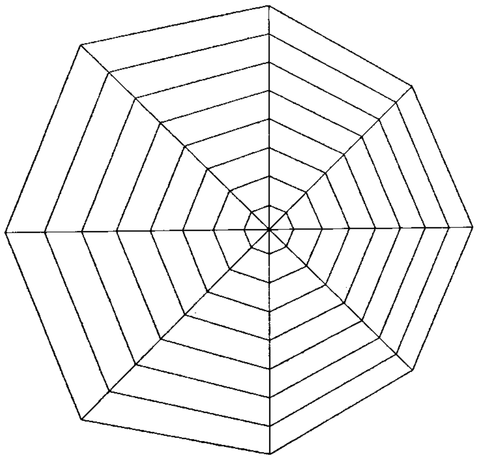

FIG. 10a (r,z) E=1

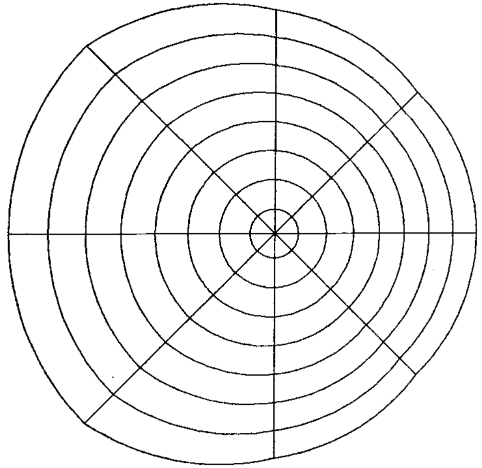

FIG. 10c (ρ,θ) E=1

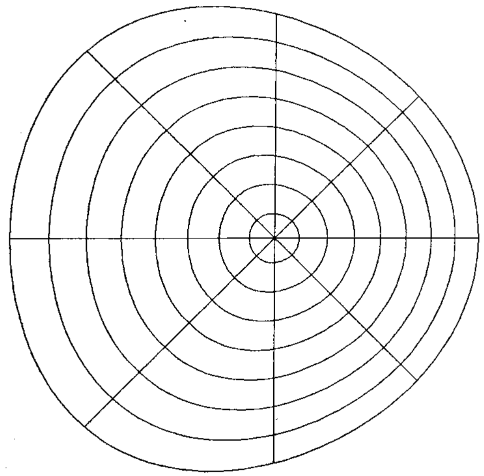

FIG. 10e (σ,θ) E=1

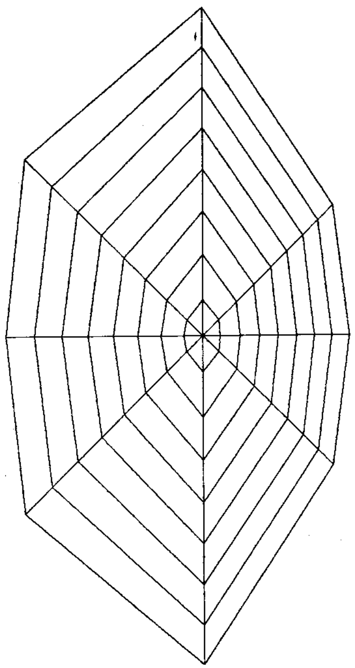

FIG. 10b (r,z) E=2

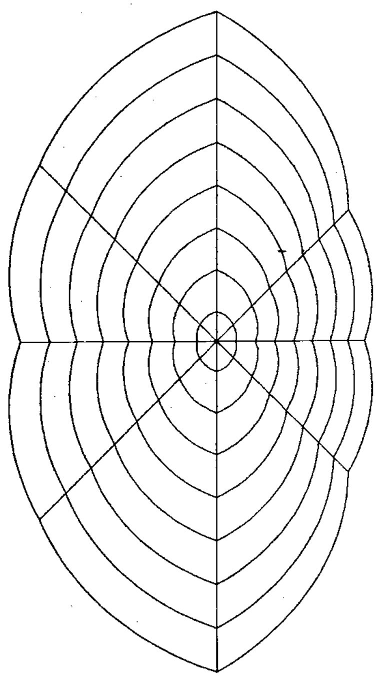

FIG. 10d (ρ,θ) E=2

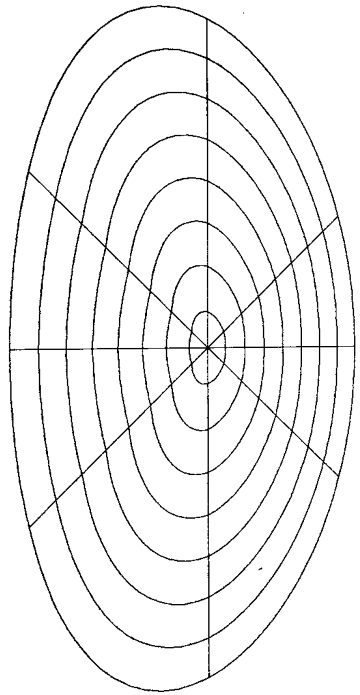

FIG. 10f (σ,θ) E=2

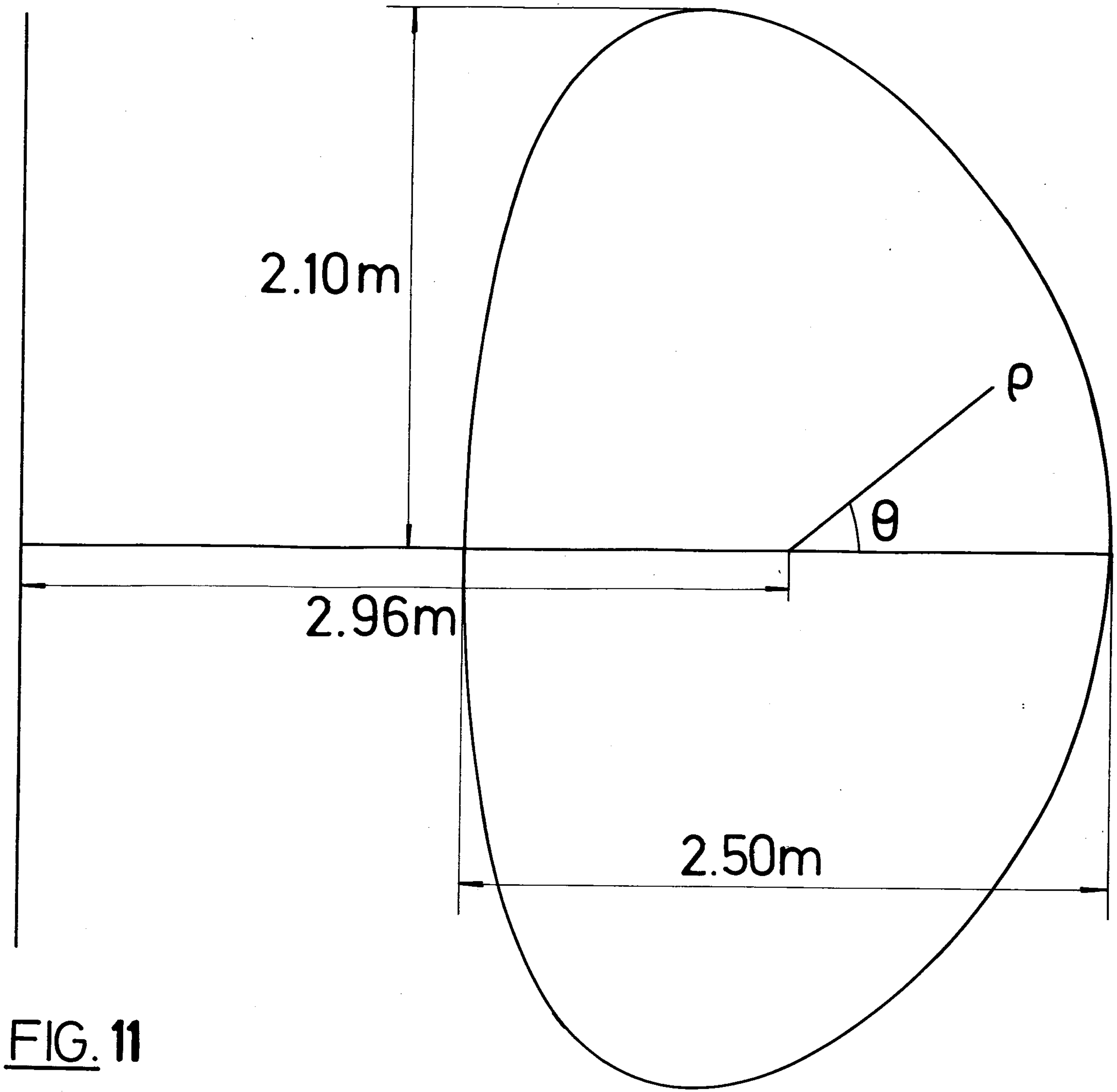

FIG. 11

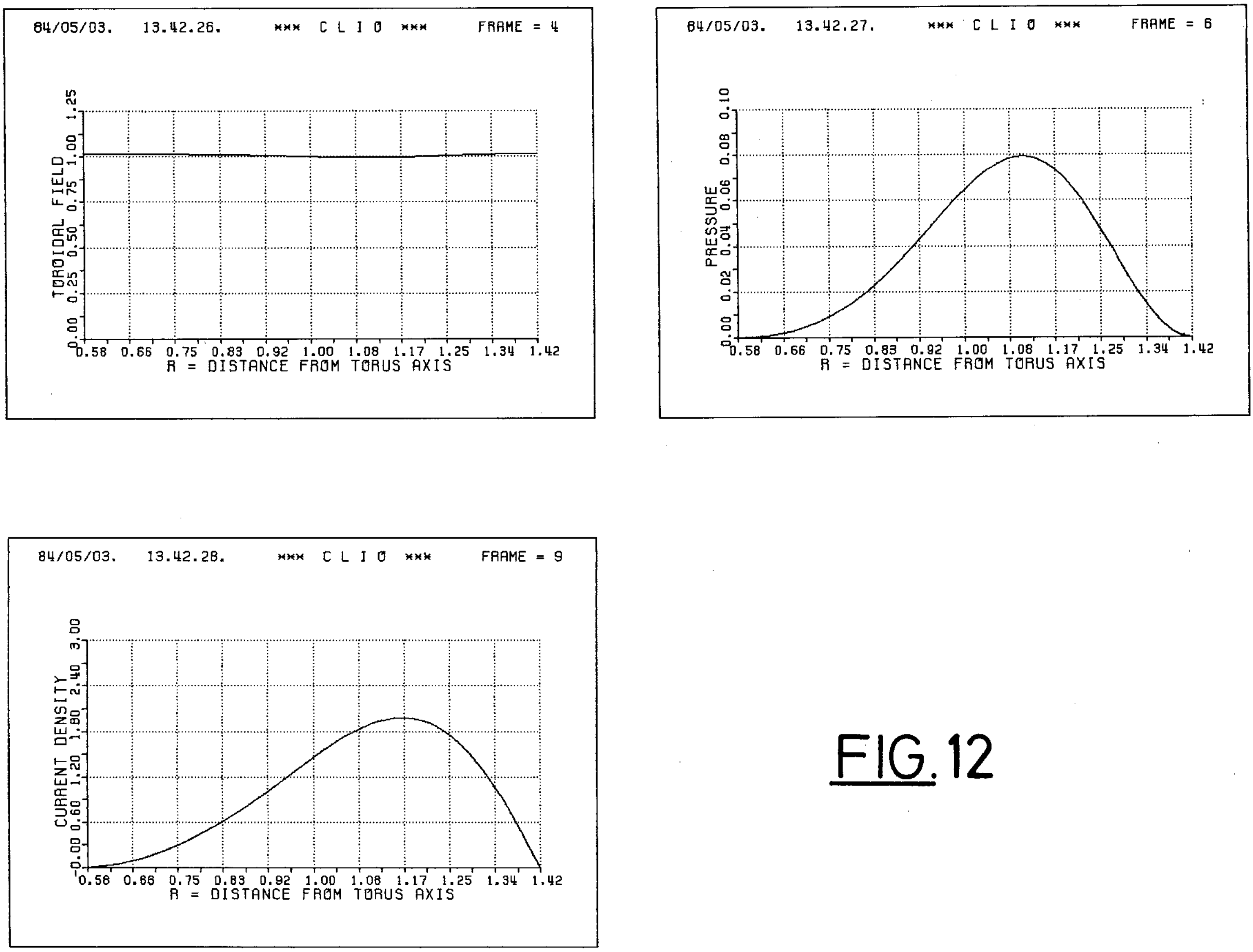
84/05/03. 13.42.26. *** C L I O *** FRAME = 4
TOROIDAL FIELD
0.00 0.25 0.50 0.75 1.00 1.25
0.58 0.66 0.75 0.83 0.92 1.00 1.08 1.17 1.25 1.34 1.42
R = DISTANCE FROM TORUS AXIS
84/05/03. 13.42.27. *** C L I O *** FRAME = 6
PRESSURE
0.00 0.02 0.04 0.06 0.08 0.10
0.58 0.66 0.75 0.83 0.92 1.00 1.08 1.17 1.25 1.34 1.42
R = DISTANCE FROM TORUS AXIS
84/05/03. 13.42.28. *** C L I O *** FRAME = 9
CURRENT DENSITY
-0.00 0.60 1.20 1.80 2.40 3.00
0.58 0.66 0.75 0.83 0.92 1.00 1.08 1.17 1.25 1.34 1.42
R = DISTANCE FROM TORUS AXIS

FIG. 12

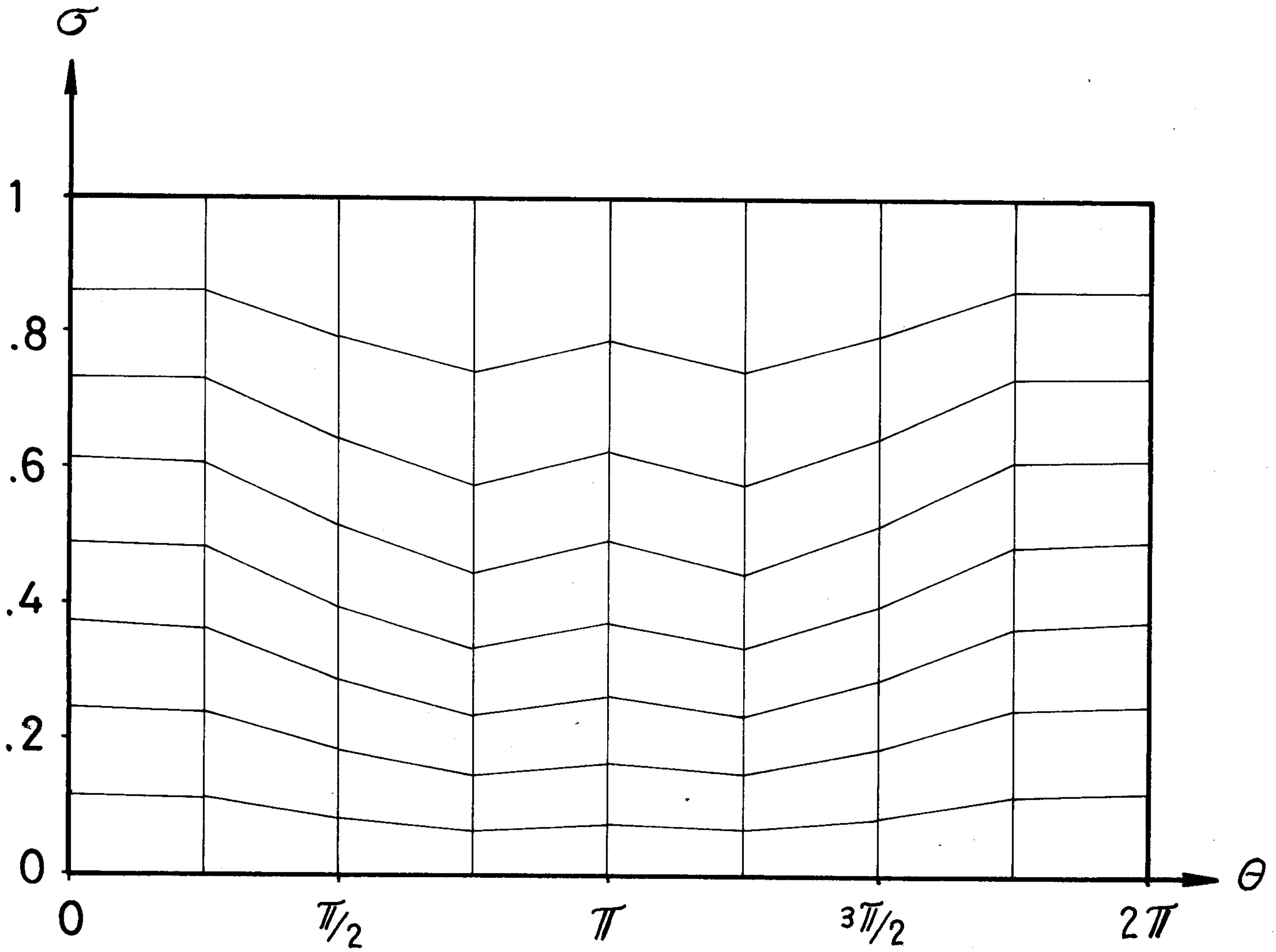

FIG. 13

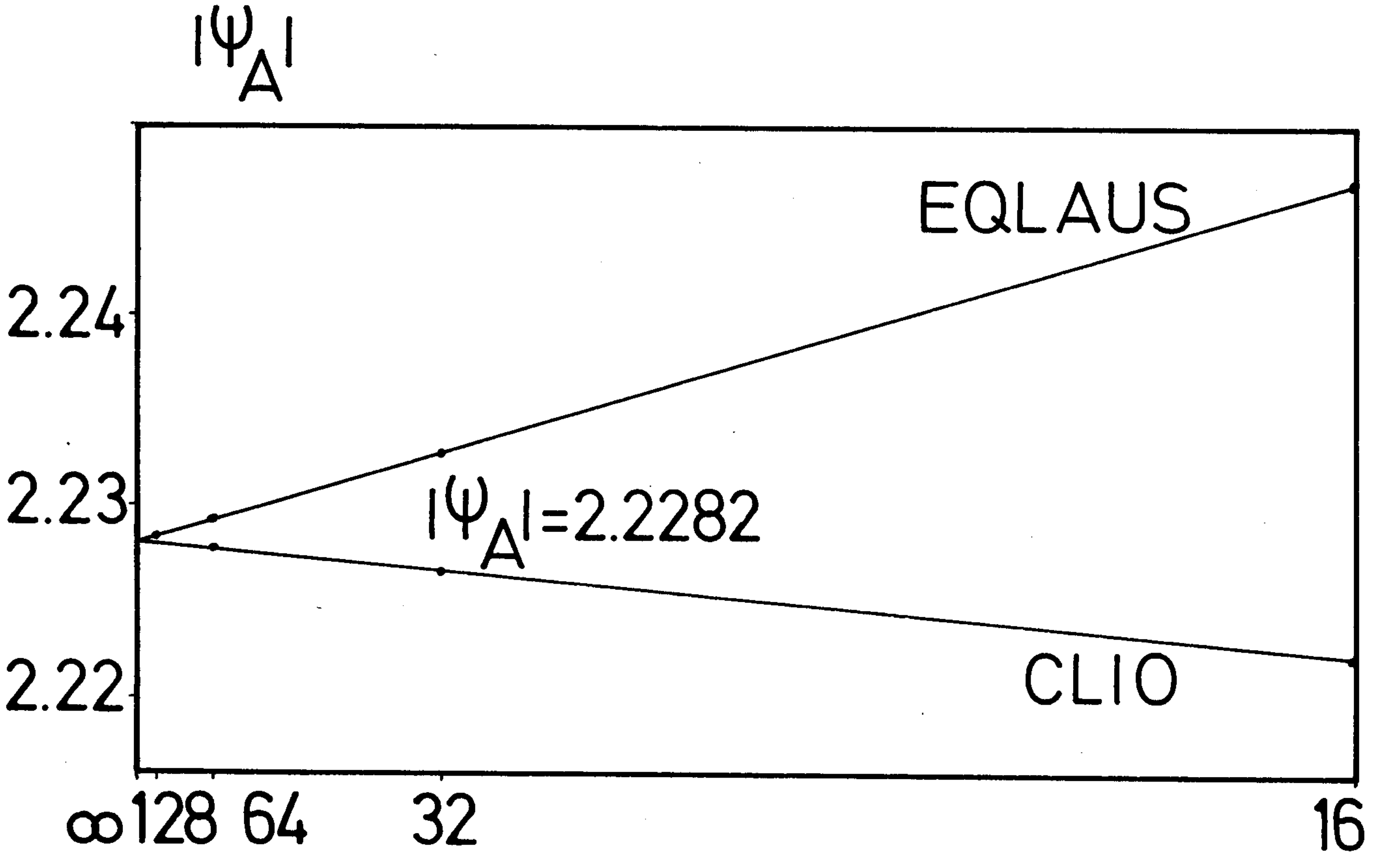

FIG. 14

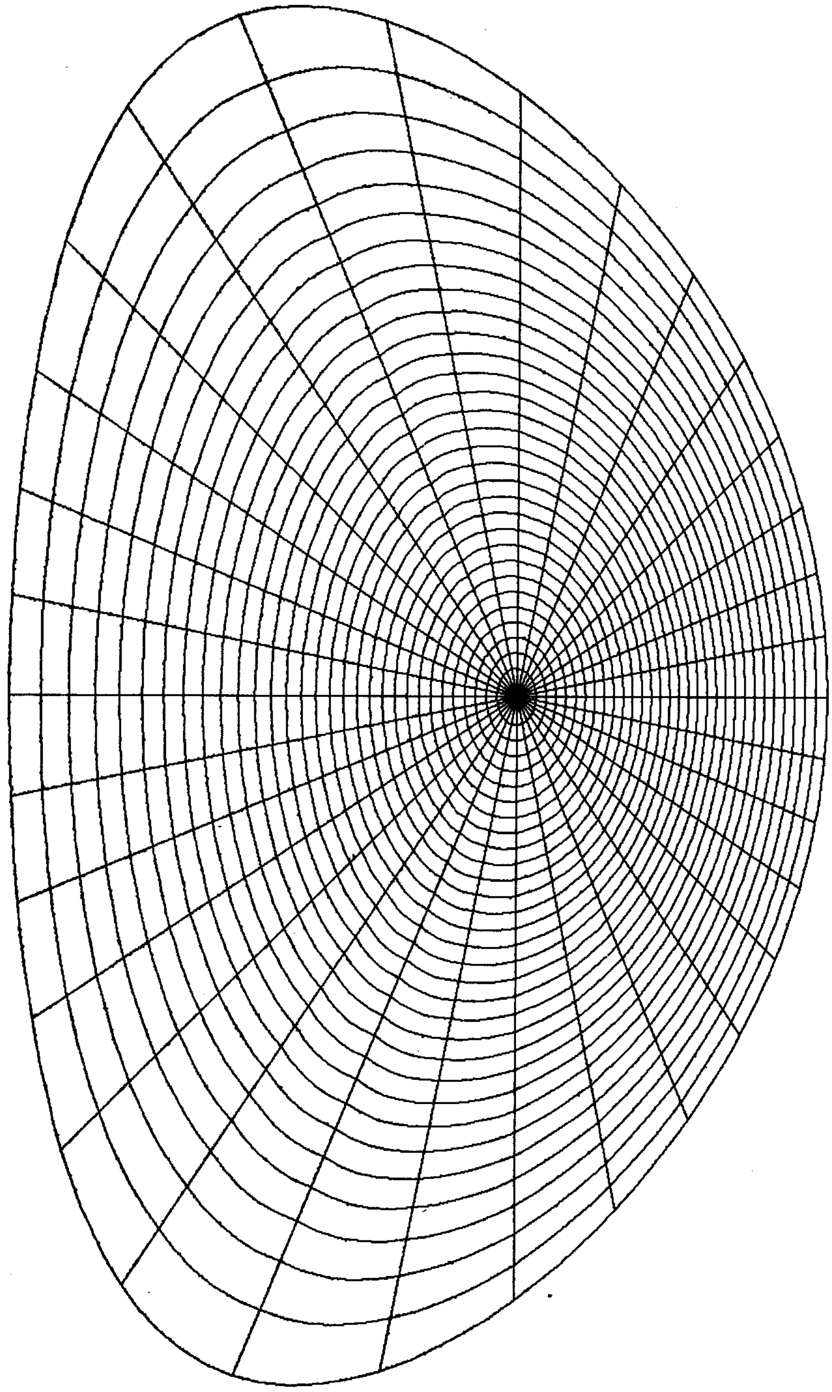

FIG. 15

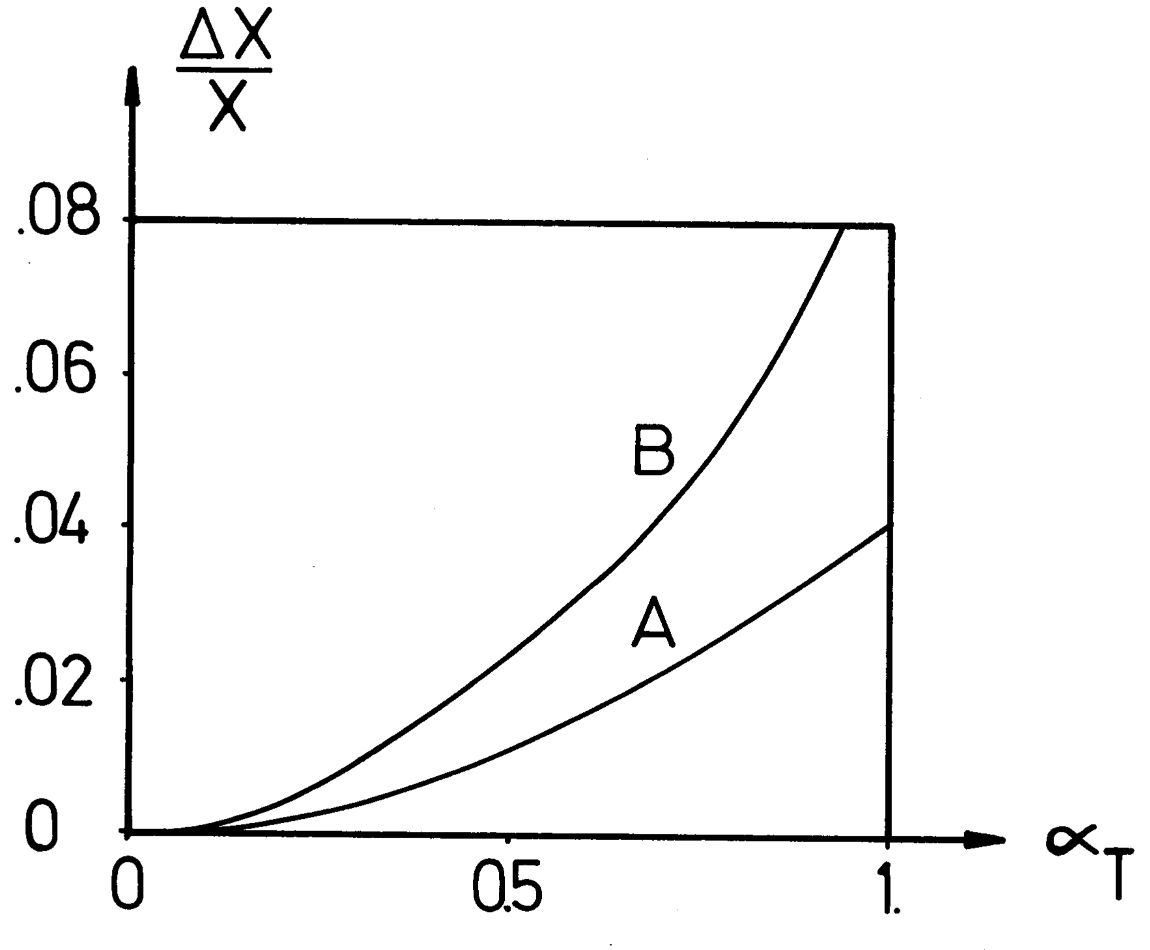

FIG. 16

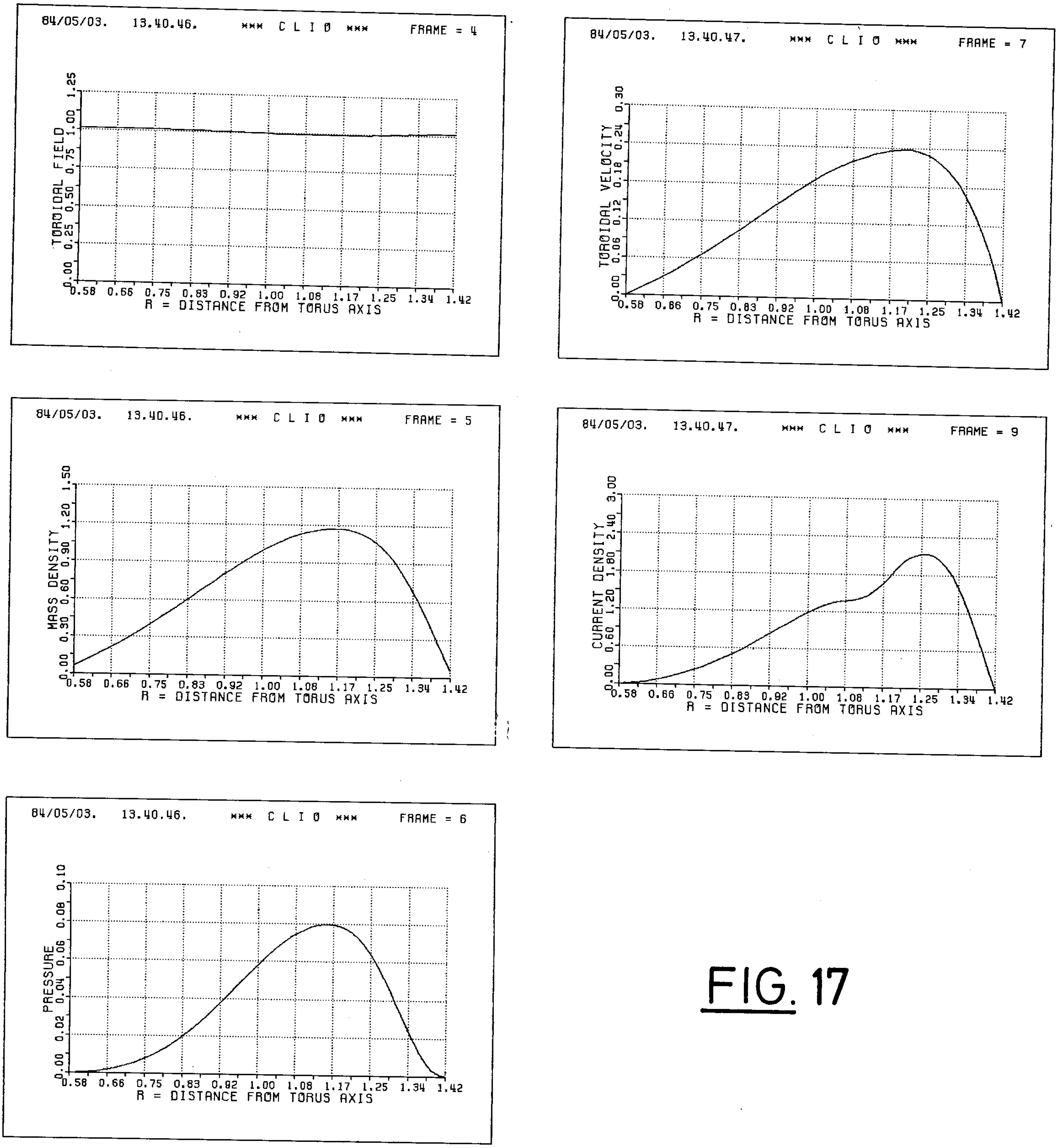
84/05/03. 13.40.46. *** C L I O *** FRAME = 4
TOROIDAL FIELD
0.00 0.25 0.50 0.75 1.00 1.25
0.58 0.66 0.75 0.83 0.92 1.00 1.08 1.17 1.25 1.34 1.42
R = DISTANCE FROM TORUS AXIS
84/05/03. 13.40.47. *** C L I O *** FRAME = 7
TOROIDAL VELOCITY
0.00 0.06 0.12 0.18 0.24 0.30
0.58 0.66 0.75 0.83 0.92 1.00 1.08 1.17 1.25 1.34 1.42
R = DISTANCE FROM TORUS AXIS
84/05/03. 13.40.46. *** C L I O *** FRAME = 5
MASS DENSITY
0.00 0.30 0.60 0.90 1.20 1.50
0.58 0.66 0.75 0.83 0.92 1.00 1.08 1.17 1.25 1.34 1.42
R = DISTANCE FROM TORUS AXIS
84/05/03. 13.40.47. *** C L I O *** FRAME = 9
CURRENT DENSITY
0.00 0.60 1.20 1.80 2.40 3.00
0.58 0.66 0.75 0.83 0.92 1.00 1.08 1.17 1.25 1.34 1.42
R = DISTANCE FROM TORUS AXIS
84/05/03. 13.40.46. *** C L I O *** FRAME = 6
PRESSURE
0.00 0.02 0.04 0.06 0.08 0.10
0.58 0.66 0.75 0.83 0.92 1.00 1.08 1.17 1.25 1.34 1.42
R = DISTANCE FROM TORUS AXIS

FIG. 17

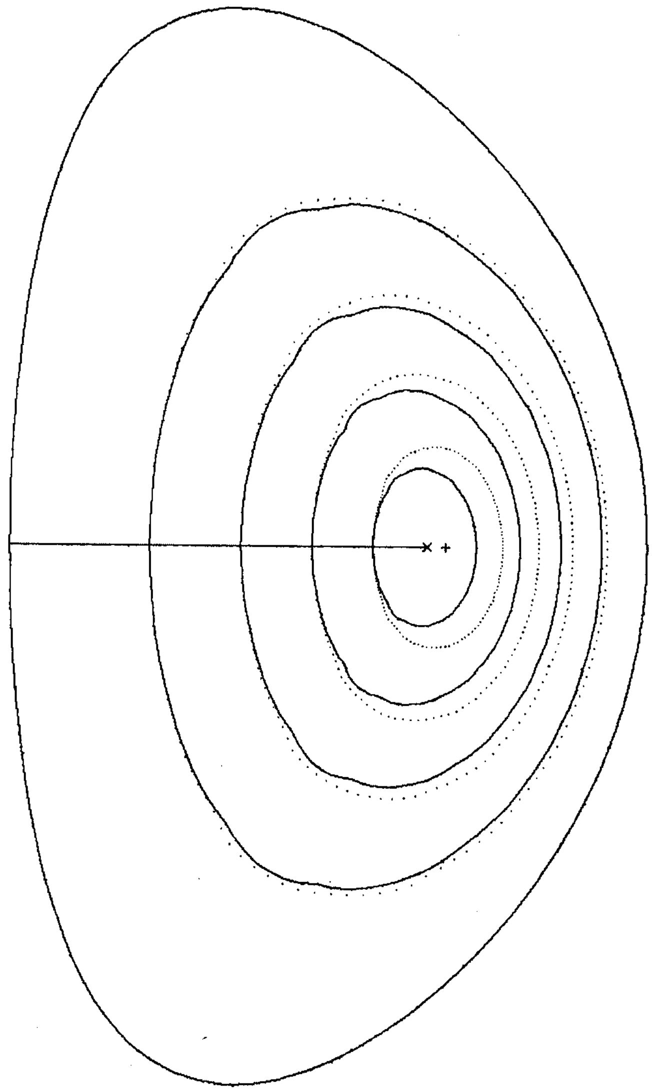

FIG. 18

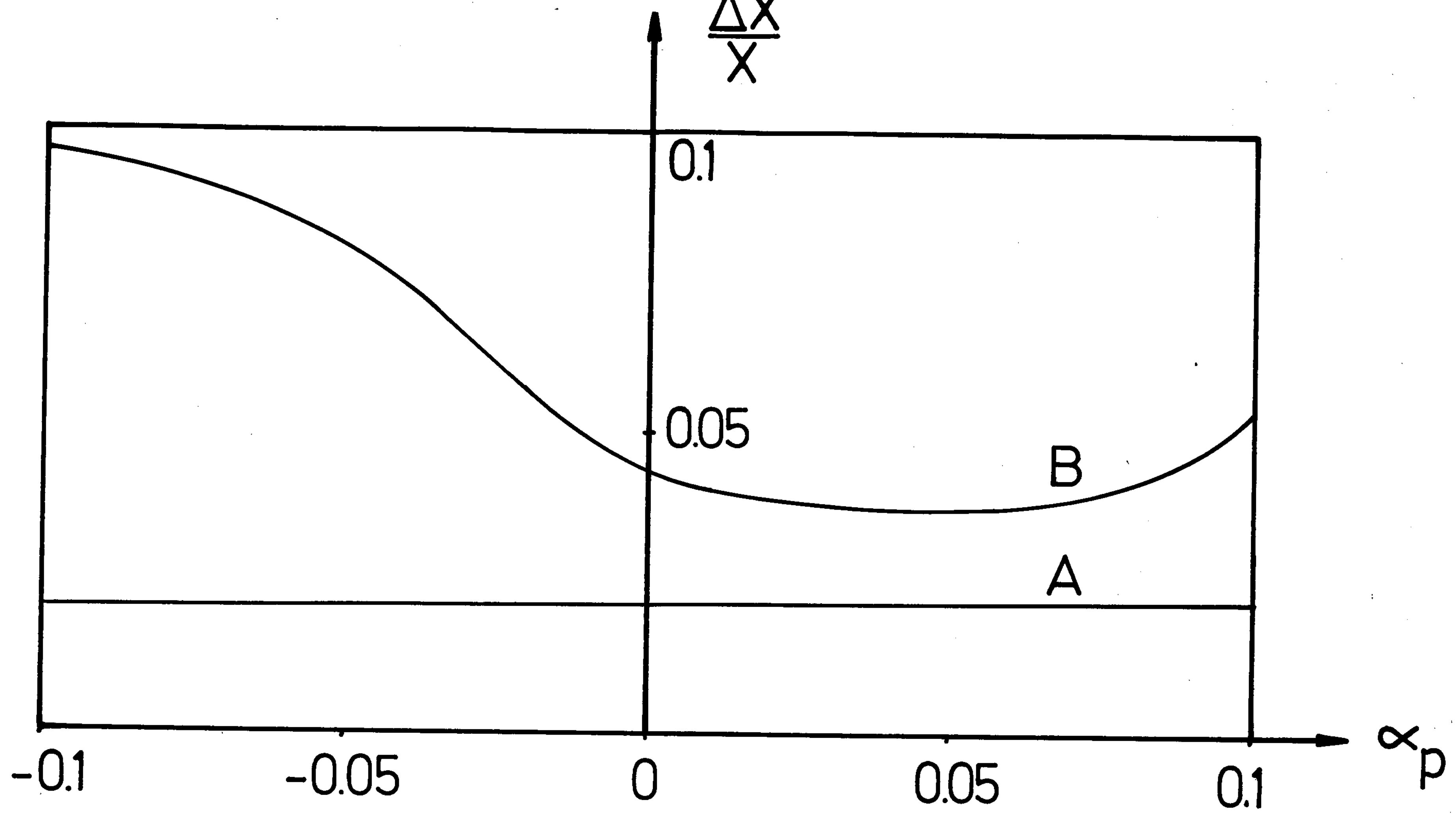

FIG. 19

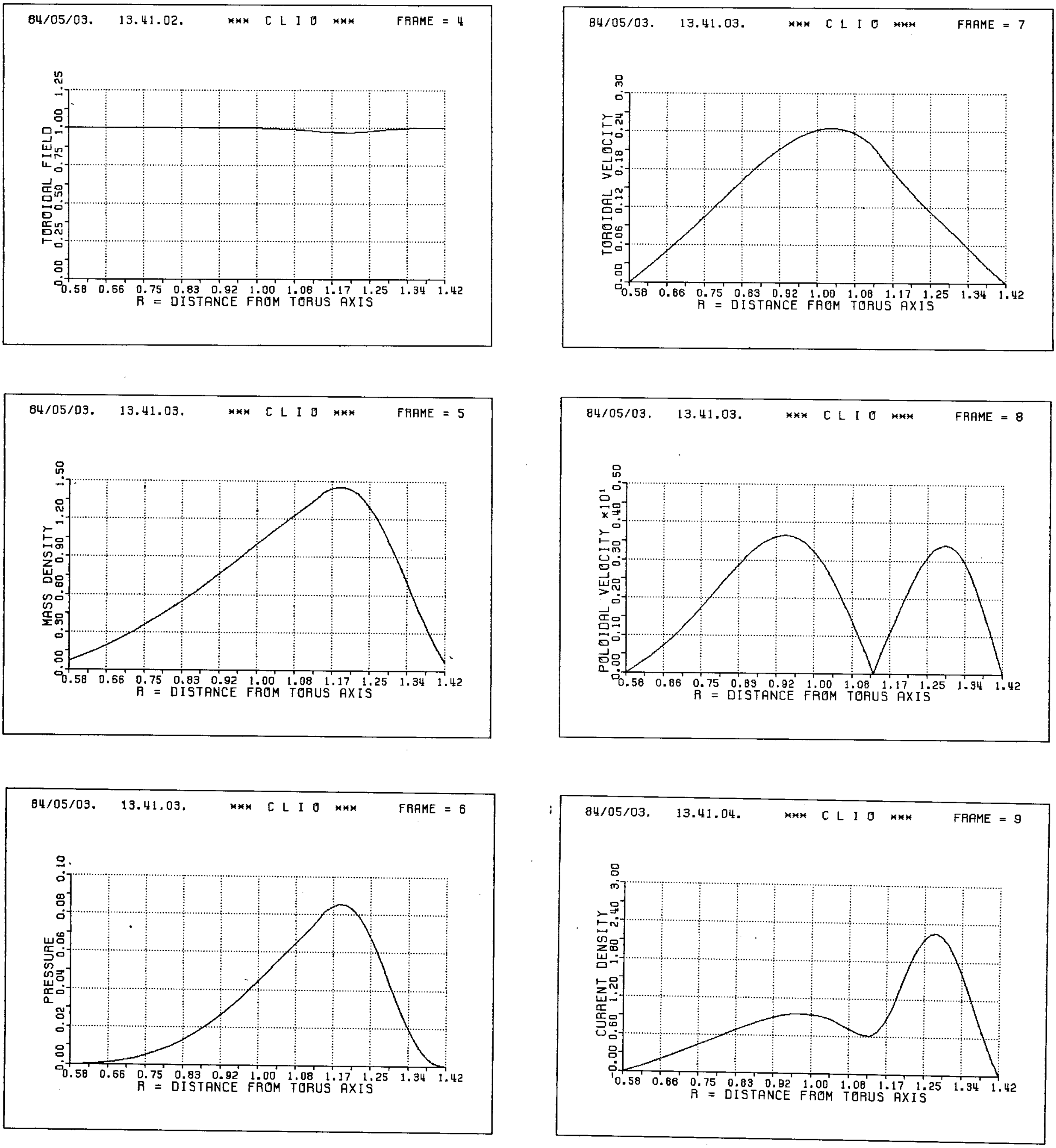
84/05/03. 13.41.02. *** C L I O *** FRAME = 4
TOROIDAL FIELD
0.00 0.25 0.50 0.75 1.00 1.25
0.58 0.66 0.75 0.83 0.92 1.00 1.08 1.17 1.25 1.34 1.42
R = DISTANCE FROM TORUS AXIS
84/05/03. 13.41.03. *** C L I O *** FRAME = 7
TOROIDAL VELOCITY
0.00 0.06 0.12 0.18 0.24 0.30
0.58 0.66 0.75 0.83 0.92 1.00 1.08 1.17 1.25 1.34 1.42
R = DISTANCE FROM TORUS AXIS
84/05/03. 13.41.03. *** C L I O *** FRAME = 5
MASS DENSITY
0.00 0.30 0.60 0.90 1.20 1.50
0.58 0.66 0.75 0.83 0.92 1.00 1.08 1.17 1.25 1.34 1.42
R = DISTANCE FROM TORUS AXIS
84/05/03. 13.41.03. *** C L I O *** FRAME = 8
POLOIDAL VELOCITY ×10¹
0.00 0.10 0.20 0.30 0.40 0.50
0.58 0.66 0.75 0.83 0.92 1.00 1.08 1.17 1.25 1.34 1.42
R = DISTANCE FROM TORUS AXIS
84/05/03. 13.41.03. *** C L I O *** FRAME = 6
PRESSURE
0.00 0.02 0.04 0.06 0.08 0.10
0.58 0.66 0.75 0.83 0.92 1.00 1.08 1.17 1.25 1.34 1.42
R = DISTANCE FROM TORUS AXIS
84/05/03. 13.41.04. *** C L I O *** FRAME = 9
CURRENT DENSITY
0.00 0.60 1.20 1.80 2.40 3.00
0.58 0.66 0.75 0.83 0.92 1.00 1.08 1.17 1.25 1.34 1.42
R = DISTANCE FROM TORUS AXIS

FIG. 20

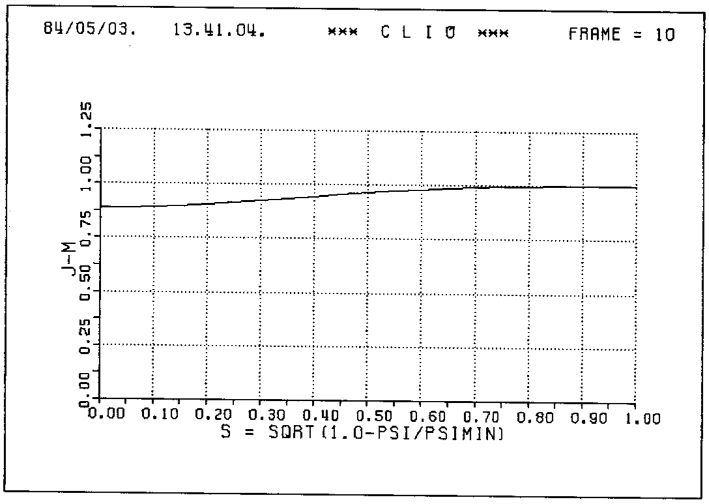
84/05/03. 13.41.04. *** C L I O *** FRAME = 10
J-M
0.00 0.25 0.50 0.75 1.00 1.25
0.00 0.10 0.20 0.30 0.40 0.50 0.60 0.70 0.80 0.90 1.00
S = SQRT(1.0-PSI/PSIMIN)

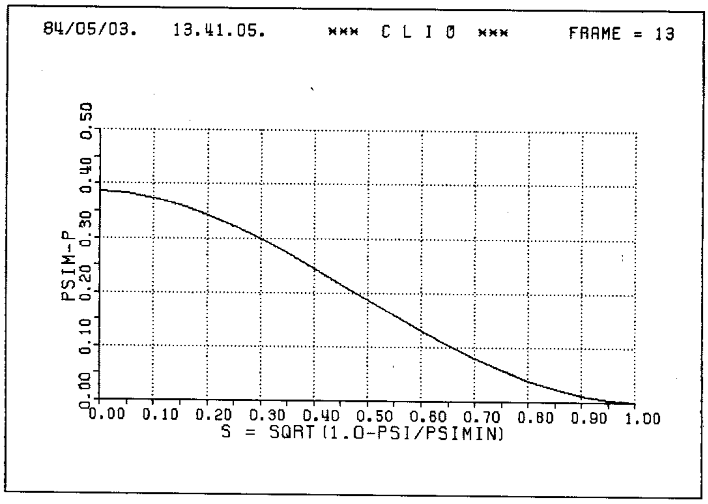
84/05/03. 13.41.05. *** C L I O *** FRAME = 13
PSIM-P
0.00 0.10 0.20 0.30 0.40 0.50
0.00 0.10 0.20 0.30 0.40 0.50 0.60 0.70 0.80 0.90 1.00
S = SQRT(1.0-PSI/PSIMIN)

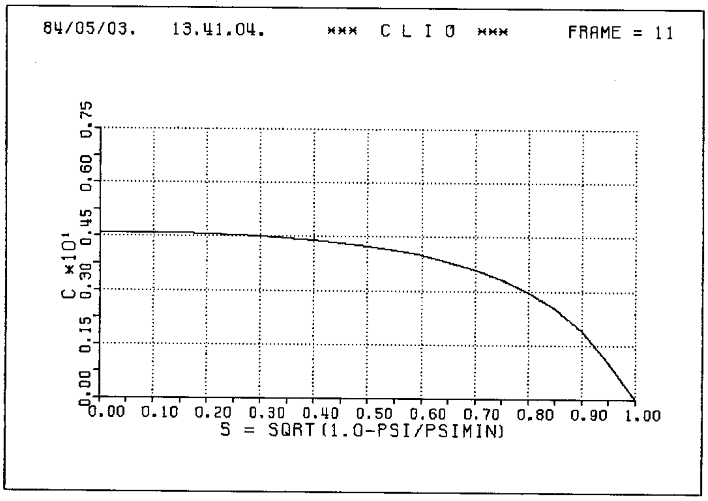
84/05/03. 13.41.04. *** C L I O *** FRAME = 11
C ×10¹
0.00 0.15 0.30 0.45 0.60 0.75
0.00 0.10 0.20 0.30 0.40 0.50 0.60 0.70 0.80 0.90 1.00
S = SQRT(1.0-PSI/PSIMIN)

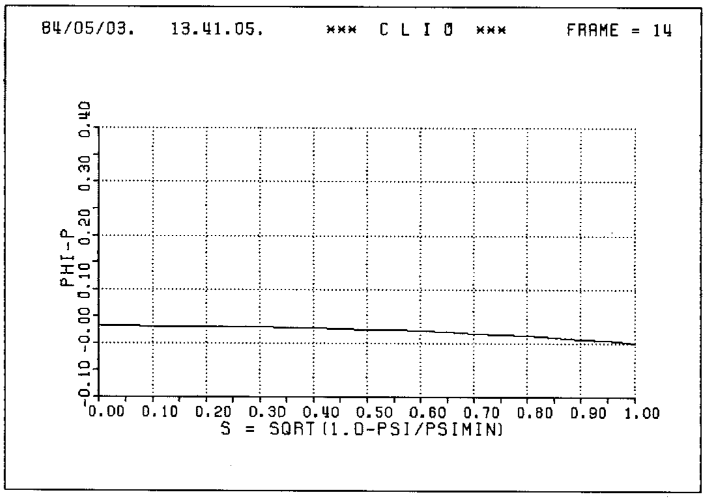
84/05/03. 13.41.05. *** C L I O *** FRAME = 14
PHI-P
-0.10 -0.00 0.10 0.20 0.30 0.40
0.00 0.10 0.20 0.30 0.40 0.50 0.60 0.70 0.80 0.90 1.00
S = SQRT(1.0-PSI/PSIMIN)

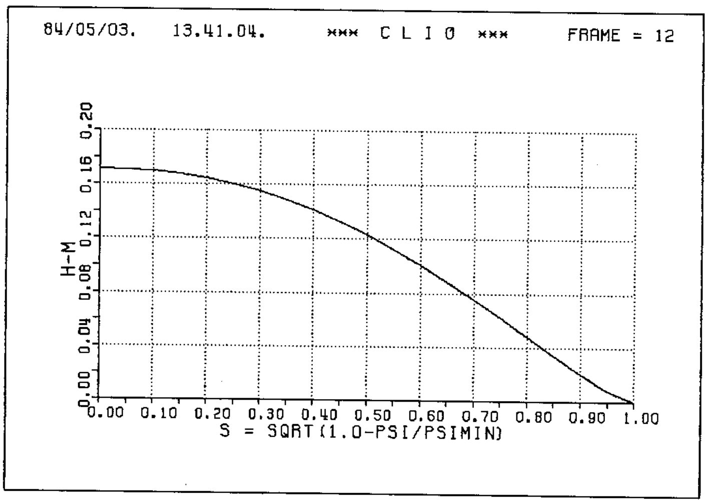
84/05/03. 13.41.04. *** C L I O *** FRAME = 12
H-M
0.00 0.04 0.08 0.12 0.16 0.20
0.00 0.10 0.20 0.30 0.40 0.50 0.60 0.70 0.80 0.90 1.00
S = SQRT(1.0-PSI/PSIMIN)

FIG. 21

Appendix A

We prove some vector analytic theorems on vector fields in cases of symmetry. By this we mean that there is a system of coordinates so that the components of the vector field under consideration and the components of the metric tensor in these coordinates are independent of an "ignorable" coordinate ϕ. Let $\underline{x}$ be the position vector with the cartesian components (x,y,z) referred to the (in general curvilinear) coordinates $u = (u^1, u^2)$ and ϕ, i.e. $\underline{x} = \underline{x}(u,\phi)$. For its partial derivatives we use the notations

$$\underline{x}_\ell = \begin{cases} \dfrac{\partial \underline{x}}{\partial u^\ell} & , \ \ell = 1,2 \\ \underline{x}_\phi = \dfrac{\partial \underline{x}}{\partial \phi} & , \ \ell = 3 \end{cases} \tag{A1}$$

For the gradients of u and ϕ, considered as functions of space, we write

$$\underline{x}^\ell = \begin{cases} \underline{\nabla} u^\ell & , \ \ell = 1,2 \\ \underline{\nabla} \phi & , \ \ell = 3 \end{cases} \tag{A2}$$

so that for the metric tensor $\underline{g}$ and for any vector field $\underline{A}$ we have the representations

$$\underline{g} = g_{k\ell}\, \underline{x}^k \underline{x}^\ell = g^{k\ell}\, \underline{x}_k \underline{x}_\ell \tag{A3}$$

$$g_{k\ell} = \underline{x}_k \cdot \underline{x}_\ell \quad , \quad g^{k\ell} = \underline{x}^k \cdot \underline{x}^\ell \tag{A4}$$

$$\underline{A} = A_\ell\, \underline{x}^\ell = A^\ell\, \underline{x}_\ell \, . \tag{A5}$$

In these formulas the usual summation convention for upper and lower indices is used. Then the following identities can be derived :

$$\underline{\nabla} \cdot \underline{x}_\phi = 0 \tag{A6}$$

$$\underline{\nabla} \times (\underline{x}_\phi \times \underline{A}) = \underline{x}_\phi \; \underline{\nabla} \cdot \underline{A} \tag{A7}$$

$$\underline{\nabla} \times \frac{\underline{x}_\phi}{g_{\phi\phi}} = \underline{x}_\phi \; \underline{\nabla} \cdot \frac{\underline{x}_\phi \times \underline{\nabla}\phi}{g_{\phi\phi}} \, . \tag{A8}$$

The action of the $\underline{\nabla}$-operator can be obtained putting

$$\underline{\nabla} = \underline{x}^{\ell} \partial_\ell \tag{A9}$$

where

$$\partial_\ell = \begin{cases} \dfrac{\partial}{\partial u^\ell} & , \ell = 1, 2 \\ \partial_\phi = \dfrac{\partial}{\partial \phi} & , \ell = 3 \; . \end{cases} \tag{A10}$$

Then (A6) follows from the sequence of equations

$$\begin{aligned} \underline{\nabla} \cdot \underline{x}_\phi &= \underline{x}^{\ell} \cdot \partial_\ell \underline{x}_\phi = \underline{x}^{\ell} \cdot \partial_\phi \underline{x}_\ell \\ &= g^{\ell k} \underline{x}_k \cdot \partial_\phi \underline{x}_\ell = \frac{1}{2} g^{\ell k} \partial_\phi g_{\ell k} = 0 . \end{aligned} \tag{A11}$$

The second equality sign is due to the equality of mixed derivatives and the third one is consequence of the symmetry of the metric tensor $\underline{g}$.

Evaluation of the left-hand side of (A7) leads to

$$\begin{aligned} \underline{\nabla} \times (\underline{x}_\phi \times \underline{A}) &= \underline{x}^{\ell} \times \partial_\ell (\underline{x}_\phi \times \underline{A}) \\ &= \underline{x}^{\ell} \times (\partial_\phi \underline{x}_\ell) \times \underline{A} + \underline{x}^{\ell} \times (\underline{x}_\phi \times \partial_\ell \underline{A}) \\ &= A^{\ell} \partial_\phi \underline{x}_\ell + \underline{x}_\phi \, \underline{x}^{\ell} \cdot \partial_\ell \underline{A} - \partial_\phi \underline{A} \\ &= \underline{x}_\phi \, \underline{x}^{\ell} \cdot \partial_\ell \underline{A} \, , \end{aligned} \tag{A12}$$

as $\partial_\phi A^1 = 0$.

Once that (A7) is proved (A8) follow easily if we put $\underline{A} = \underline{x}_\phi \times \underline{\nabla}\phi / g_{\phi\phi}$ and then invoke (A7) :

$$\underline{\nabla} \times \left[\underline{x}_\phi \times \frac{\underline{x}_\phi \times \underline{\nabla}\phi}{g_{\phi\phi}} \right] = \underline{\nabla} \times \frac{\underline{x}_\phi}{g_{\phi\phi}} = \underline{x}_\phi \, \underline{\nabla} \cdot \frac{\underline{x}_\phi \times \underline{\nabla}\phi}{g_{\phi\phi}} \tag{A13}$$

as $\underline{x}_\phi \cdot \underline{\nabla}\phi = 1$ and $\underline{x}_\phi \cdot \underline{x}_\phi = g_{\phi\phi}$ by definition.

For a divergence-free vector field $\underline{B}$ we find the further relation

$$\underline{\nabla} \cdot \left[\alpha \, \underline{x}_\phi \times (\underline{B} \times \underline{x}_\phi) \right] = \underline{B} \cdot \underline{\nabla} (\alpha \, g_{\phi\phi}) \, . \tag{A14}$$

Here the step-by-step proof is

$$\underline{\nabla}\cdot\left[\alpha\,\underline{x}_\phi\times(\underline{B}\times\underline{x}_\phi)\right] = (\underline{B}\times\underline{x}_\phi)\cdot\underline{\nabla}\times(\alpha\,\underline{x}_\phi)$$
$$= \underline{B}\cdot\left[\underline{x}_\phi\times\underline{\nabla}\times(\alpha\,\underline{x}_\phi)\right] = \underline{B}\cdot\left[\underline{x}_\phi\times\underline{\nabla}\times\left(\alpha\, g_{\phi\phi}\frac{\underline{x}_\phi}{g_{\phi\phi}}\right)\right] \tag{A15}$$
$$= \underline{B}\cdot\left\{\underline{x}_\phi\times\left[\underline{\nabla}(\alpha\, g_{\phi\phi})\times\frac{\underline{x}_\phi}{g_{\phi\phi}}\right]\right\}$$
$$= \underline{B}\cdot\underline{\nabla}(\alpha\, g_{\phi\phi})\,.$$

Now we apply the derived theorems to the equations (2.9) to (2.13).

(2.10) and (2.11) together with (A6) give the general forms of (2.15) and (2.16) :

$$\underline{B} = \frac{1}{g_{\phi\phi}}\left(\underline{x}_\phi\times\underline{\nabla}\psi + J\,\underline{x}_\phi\right)\,, \quad J \equiv B_\phi = \underline{B}\cdot\underline{x}_\phi \tag{A16}$$

$$\rho\underline{v} = \frac{1}{g_{\phi\phi}}\left(\underline{x}_\phi\times\underline{\nabla}\psi_M + L\,\underline{x}_\phi\right)\,, \quad L \equiv \rho v_\phi = \rho\underline{v}\cdot\underline{x}_\phi \tag{A17}$$

(2.22) becomes

$$L = \psi_M'\, J - \rho\, g_{\phi\phi}\,\Phi'\,. \tag{A19}$$

As to the equations of motion the components parallel to $\underline{B}$ and in the direction of $\underline{x}_\phi$ have the form of magnetic differential equations which can be integrated along field lines. This structure is due to the identity (A14). The corresponding surface quantities connected with these integrations are in the considered general geometry

$$H_M(\psi) = \frac{1}{2}\left(\frac{\psi_M' B}{\rho}\right)^2 - \frac{1}{2}\, g_{\phi\phi}\,\Phi'^2 + \mathcal{H}(S,p) \tag{A20}$$

$$J_M(\psi) = J\,D + g_{\phi\phi}\,\psi_M'\,\Phi'\,, \quad D = 1 - \frac{\psi_M'^2}{\rho}\,. \tag{A21}$$

Finally, the normal component of the equation of motion (2.43) and the subsequent equations (2.44) to (2.46) after some algebra with repeated application of the curl-formula (A7) have the general form

$$\underline{\nabla}\cdot\left[D\,\frac{\underline{\nabla}\psi}{g_{\phi\phi}}\right] + \frac{J}{g_{\phi\phi}}\,J_M' + J_M\,\underline{\nabla}\cdot\frac{\underline{x}_\phi\times\underline{\nabla}\phi}{g_{\phi\phi}} + \rho\left(H_M' - TS'\right) + (\underline{v}\cdot\underline{B})\,\psi_M'' - L\,\Phi'' = 0 \tag{A22}$$

with

$$J = \frac{J_M - g_{\phi\phi}\, \Phi' \psi_M'}{D} \tag{A23}$$

$$L = \psi_M' J - \rho\, g_{\phi\phi}\, \Phi' \tag{A24}$$

$$\underline{v} \cdot \underline{B} = \frac{1}{\rho\, g_{\phi\phi}} \left(\psi_M' |\underline{\nabla} \psi|^2 + JL \right) . \tag{A25}$$

For the mass density equation (2.41)

$$H_M - \frac{1}{2} \left(|\underline{\nabla} \psi|^2 + J^2 \right) \frac{\psi_M'^2}{\rho^2 g_{\phi\phi}} + \frac{1}{2}\, g_{\phi\phi}\, \Phi'^2 - \mathcal{H}(S, p(S,\rho)) = 0 \tag{A26}$$

is obtained.

Appendix B

	MKSA-Unit	Quantity (MKSA)	= Factor	. Quantity (N.U.)	N.U.
Velocity	m/s	v^*	c	v	1
Poloidal Mass Flux	kg/s	Ψ_M^*	$1/c$	Ψ_M	J/m
Hydrodynamic Circulation	kg/(ms)	L^*	$1/c$	L	J/m^2
Electric Potential	V	Φ^*	$1/\varepsilon_o^{1/2}$	Φ	$(J/m)^{1/2}$
Magnetic Induction	T	B^*	$\mu_o^{1/2}$	B	$(J/m^3)^{1/2}$
Poloidal Magnetic Flux	Vs	Ψ^*	$\mu_o^{1/2}$	Ψ	$(J/m^3)^{1/2}$
Current Density	A/m^2	j^*	$1/\mu_o^{1/2}$	j	$(J/m^2)^{1/2}$
Poloidal Current	A	J^*, J_M^*	$1/\mu_o^{1/2}$	J, J_M	$(J/m)^{1/2}$
Toroidal Current	A	I^*	$1/\mu_o^{1/2}$	I	$(J/m)^{1/2}$
Specific Entropy	J/(kg.deg(K))	S^*	kc^2	S	1/J
Entropy Constant	$Jm^{3(\gamma-1)}/kg^{\gamma}$	C^*	$c^{2\gamma}$	C	$(m^3/J)^{\gamma-1}$
Specific Enthalpy	J/kg	H^*, H_M^*	c^2	H, H_M	1
Specific Free Enthalpy	J/kg	G^*	c^2	G	1
Specific Internal Energy	J/kg	U^*	c^2	U	1
Pressure	J/m^3	p^*	1	p	J/m^3
Mass Density	kg/m^3	ϱ^*	$1/c^2$	ϱ	J/m^3
Absolute Temperature	deg(K)	T^*	$1/k$	T	J